

2010

# Electrospinning protein nanofibers to control cell adhesion

Cynthia Chinwe Nwachukwu  
*University of South Florida*

Follow this and additional works at: <http://scholarcommons.usf.edu/etd>

 Part of the [American Studies Commons](#)

---

## Scholar Commons Citation

Nwachukwu, Cynthia Chinwe, "Electrospinning protein nanofibers to control cell adhesion" (2010). *Graduate Theses and Dissertations*.  
<http://scholarcommons.usf.edu/etd/1727>

This Thesis is brought to you for free and open access by the Graduate School at Scholar Commons. It has been accepted for inclusion in Graduate Theses and Dissertations by an authorized administrator of Scholar Commons. For more information, please contact [scholarcommons@usf.edu](mailto:scholarcommons@usf.edu).

Electrospinning Protein Nanofibers to Control Cell Adhesion

by

Cynthia Chinwe Nwachukwu

A thesis submitted in partial fulfillment  
of the requirements for the degree of  
Master of Science in Biomedical Engineering  
Department of Chemical and Biomedical Engineering  
College of Engineering  
University of South Florida

Major Professor: Nathan D. Gallant, Ph.D.  
William E. Lee, Ph.D.  
Ryan Toomey, Ph.D.

Date of Approval:  
June 29, 2010

Keywords: Bovine Albumin Serum, Focal Adhesion, Fibronectin,  
Globular Proteins, Integrins

Copyright © 2010, Cynthia Chinwe Nwachukwu

## **DEDICATION**

I would like to dedicate this thesis to my parents Magnus C. Nwachukwu-O and MaryJane A. Nwachukwu-O, my brother Santos and sisters Sandra and Cindy whose prayers strength, support and guidance has made me who I am today and who I will become. I could not have done it without you.

## **ACKNOWLEDGEMENTS**

I would also like to offer a special thanks to my advisor Nathan D. Gallant for taking a chance on me. Your motivation and guidance has seen me through and I am honored to have been blessed with a teacher such as you. I would like to thank Dr. William Lee and Dr. Ashok Kumar for serving on my thesis committee and providing me with valuable feedback to help finalize my manuscript. I would also like to thank Mr. Kranthi Elineni a Ph.D. student at the University of South Florida and member of my lab for your lab and advice throughout my research.

## TABLE OF CONTENTS

LIST OF TABLES .....	iii
LIST OF FIGURES .....	v
ABSTRACT .....	vii
CHAPTER 1: INTRODUCTION .....	1
1.1 BACKGROUND AND MOTIVATION .....	1
1.2 ELECTROSPINNING HISTORY .....	4
1.3 PROCESSING PARAMETERS .....	8
1.3.1 Applied Voltage .....	9
1.3.2 Flow Rate .....	10
1.3.3 Capillary to Target Distance .....	11
1.3.4 Polymer Concentration .....	11
1.3.5 Conductivity of Solution .....	12
1.3.6 Volatility of Solution .....	12
1.4 INTEGRIN-MEDIATED CELL ADHESION .....	13
1.5 PROJECT SIGNIFICANCE .....	14
1.6 CONCLUSION AND CHAPTER OBJECTIVES .....	15
CHAPTER 2: ELECTROSPINNING DEGRADABLE NANOFIBROUS SCAFFOLDS FOR TISSUE ENGINEERING FROM GLOBULAR PROTEINS THAT REGULATE CELL ADHESION .....	16
2.1 INTRODUCTION .....	16
2.2 MATERIALS AND METHODS .....	19
2.2.1 Materials and Solutions .....	19
2.2.2 Electrospinning .....	20
2.3 EXPERIMENTAL OVERVIEW .....	21
2.3.1 Effect of Solvent on Fiber Morphology .....	23
2.3.2 Effect of Concentration .....	25
2.3.3 Effect of Flow Rate .....	27
2.3.4 Effect of C-TD Distance .....	28
2.3.5 Effect of Applied Voltage .....	31
2.3.6 Effect of Temperature .....	31

2.4 EQUIPMENTS .....	33
2.5 CONCLUSION.....	33
CHAPTER 3: CHARACTERIZATION OF FIBRONECTIN AVAILABILITY AND BIOACTIVITY UNDER THE CONDITIONS OF ELECTROSPUN SCAFFOLD FABRICATION .....	36
3.1 FIBRONECTIN .....	36
3.2 MATERIALS AND METHODS.....	37
3.2.1 Statistical Analysis of Variance (ANOVA) .....	37
3.2.2 Antibodies .....	38
3.2.3 Surface Coating with BSA and Fibronectin.....	38
3.2.4 Elisa.....	38
3.3 RESULTS .....	39
3.3.1 Fibronectin Analysis .....	39
3.3.2 (TRIAL 1) Staining for Fibronectin in Electrospun Fibers.....	39
3.3.2.1 (TRIAL 1) Results.....	40
3.3.3 (TRIAL 2) Staining for Fibronectin in BSA Films .....	42
3.3.3.1 (TRIAL 2) Results.....	43
3.3.4 (TRIAL 3) Fibronectin Staining in BSA Films, Solvent Effect on Polyclonal FN Antibody and on Monoclonal HFN7.1 Antibody Binding and Results .....	43
3.4 CONCLUSION.....	52
CHAPTER 4: CELL ADHESION AND SPREADING ON SCAFFOLDS .....	54
4.1 INTRODUCTION.....	54
4.2 MATERIALS AND METHODS.....	55
4.2.1 Cell Line and Culture Methods .....	55
4.2.2 Cell Counting.....	56
4.2.3 Cell Staining .....	56
4.3 RESULTS AND DISCUSSION.....	57
4.4 CONCLUSION.....	65
CHAPTER 5: PROJECT SUMMARY AND FUTURE CONSIDERATION.....	66
REFERENCES.....	70

## LIST OF TABLES

TABLE 2.1: Chemical properties of materials .....	20
TABLE 2.2: Original process parameter .....	23
TABLE 2.3: Fiber diameter measurement analysis to illustrate the relationship between concentration of electrospun BSA and fiber dimensions .....	26
TABLE 2.4: Fiber diameter measurement analysis to illustrate the relationship between flow rate of electrospun BSA and fiber dimensions .....	28
TABLE 2.5: Electrospun 12% BSA fiber with differing distance and mat characteristics .....	30
TABLE 2.6: Temperature (°C ) vs. reaction time (hr).....	32
TABLE 2.7: Composition of FN incorporated into optimized parameter from electrospun fibers .....	34
TABLE 2.8: Summary of the effect of the different processing parameters .....	35
TABLE 3.1: Trial 1 FN absorbance data.....	40
TABLE 3.2: Anova: Single factor analysis of TFE/H <sub>2</sub> O solvent effect on polyclonal FN antibody binding .....	47
TABLE 3.3 Anova: Single factor analysis of the PBS solvent effect on polyclonal FN antibody binding .....	47
TABLE 3.4: Anova: Single factor analysis of TFE/H <sub>2</sub> O solvent effect on HFN7.1 antibody binding .....	49
TABLE 3.5: Anova: Single factor analysis of PBS solvent effect on HFN7.1 antibody binding .....	49

TABLE 3.6: Anova: Single factor analysis of TFE/H<sub>2</sub>O solvent effect on polyclonal FN antibody binding on BSA fibers .....50

TABLE 3.7: Anova: Single factor analysis of TFE/H<sub>2</sub>O solvent effect on HFN7.1 antibody binding on BSA fibers .....51

## LIST OF FIGURES

FIGURE 1.1: Schematic of the electrospinning setup.....	4
FIGURE 1.2: Diagrammatic representation of successive jet instabilities causing elongation and thinning.....	6
FIGURE 1.3: Diagram showing the instantaneous position of the path of an electrospinning jet that contained three successive electrical bending instabilities.....	7
FIGURE 1.4: Beads created during electrospinning .....	9
FIGURE 1.5: Effect of varying the applied voltage on the formation of the Taylor cone .....	10
FIGURE 2.1: Aluminum foil covered target plate (blue) with cover slips (white) to collect electrospun fibers .....	21
FIGURE 2.2: Mathematical calculation of electrospun materials .....	23
FIGURE 2.3: Comparison of BSA fibers with and without addition of $\beta$ -mercaptoethanol (a) without (b) with (10x).....	24
FIGURE 2.4: Effect of BSA concentration on fiber diameter (a) 10% BSA, (b) 15% BSA (10x) .....	25
FIGURE 2.5: Fiber diameter measurement analysis to illustrate the relationship between concentration of electrospun BSA and fiber dimensions.....	26
FIGURE 2.6: Effect of flow rate on fiber diameter on fiber diameter at 12% concentration, 12cm (a) 0.25ml/hr flow rate (b) 1.0ml/hr (10x).....	27
FIGURE 2.7: Summary of the effect of flow rate to fiber diameter .....	28
FIGURE 2.8: Effect of collecting distance on the fiber diameter at 12% BSA (a)12cm (b) 20 cm (40x).....	29

FIGURE 2.9: Effect of collecting distance on lower concentration BSA (10%) showing blobs (40x) .....	29
FIGURE 2.10: Summary of the effect of capillary to target distance .....	30
FIGURE 3.1: Fibronectin bound to integrin at the cell surface .....	37
FIGURE 3.2: 6-well plate of BSA films (top column) and BSA fibers (bottom column) of differing FN concentration.....	42
FIGURE 3.3: Solvent effect on polyclonal FN antibody binding.....	46
FIGURE 3.4: Solvent effect on HFN7.1 antibody binding .....	48
FIGURE 3.5: TFE/H <sub>2</sub> O solvent effect on polyclonal FN antibody binding on BSA fibers.....	50
FIGURE 3.6: TFE/H <sub>2</sub> O solvent effect on polyclonal FN antibody binding on HFN7.1 antibody binding .....	51
FIGURE 4.1(a): NIH/3T3 cells adhering to BSA film (TFE/H <sub>2</sub> O solvent) with 0μg/ml FN (10x) .....	59
FIGURE 4.1(b): NIH/3T3 cells adhering to BSA film (TFE/H <sub>2</sub> O solvent) with 1μg/ml FN.....	60
FIGURE 4.1(c): NIH/3T3 cells adhering to BSA film (TFE/H <sub>2</sub> O solvent) with 10μg/ml FN.....	60
FIGURE 4.2 (a): NIH/3T3 cells adhering to BSA film (PBS solvent) with 0μg/ml FN.....	61
FIGURE 4.2 (b): NIH/3T3 cells adhering to BSA film (PBS solvent) with 1μg/ml FN.....	61
FIGURE 4.2 (c): NIH/3T3 cells adhering to BSA film (PBS solvent) with 10μg/ml FN.....	62
FIGURE 4.3: NIH/3T3 cells adhering to 10μg/ml FN film diluted in TFE/H <sub>2</sub> O solvent (10x) .....	63
FIGURE 4.4: NIH/3T3 cells adhering to BSA fibers (TFE/H <sub>2</sub> O solvent) (10x).....	64

## **Electrospinning Protein Nanofibers to Control Cell Adhesion**

**Cynthia Chinwe Nwachukwu**

### **ABSTRACT**

The structural and mechanical properties of a surface often play an integral part in the determination of the cell adhesion strength and design parameters for creating a biodegradable electrospun scaffold. Nanofibers composed of the globular proteins bovine serum albumin (BSA) and fibronectin were produced by electrospinning with the electrospun protein scaffold serving as an extracellular matrix to which adhesion interaction will exist with cells via cell surface integrin. This interaction is vital in regulation cell differentiation, growth and migration and cell adhesion.

We will demonstrate the ability to manipulate ligand-receptor interaction, the properties of the electrospun fibers, control and the formation of focal adhesions sites in cells cultured on the fibers with the ultimate goal of developing a biomimetic scaffold to investigate how cell adhesion molecules modulate cell behavior in a 3-dimensional culture.

## **CHAPTER 1: INTRODUCTION**

### **1.1 BACKGROUND AND MOTIVATION**

Cell adhesion to extracellular matrices (ECM) is essential to survival, differentiation and cell cycle regulation and plays a vital role in the function, repair and development of tissues (De Arcangelis, A. and Georges-Labouesse, E., 2000). Cell adhesion is a complex biological process that involves receptor-ligands binding, stabilization by the actin cytoskeleton, and assembly of large intracellular protein complexes known as focal adhesions. Cell-ECM adhesion is primarily mediated by the integrin family of transmembrane receptors. Integrin-mediated adhesion to ECM proteins such as fibronectin and laminin, anchors cells to the ECM, provides structure to tissues, and triggers signals that control cell migration and survival. Following the mechanical linkage, integrin cluster together and associate with the actin cytoskeleton to form focal adhesions. Focal adhesions are protein complexes that function to connect the extracellular matrix to the cell's cytoskeleton which triggers signaling pathways that directs cell response.

Our studies involving electrospun nanofibers concentrated on their use for tissue engineering shows how cell adhesion plays a significant role in this field. This aims in the production of tissue substitutes from biodegradable and biocompatible polymers and cell that are specific for the tissues. The overall goals of this project are to develop a

biomimetic scaffold and investigate how cell adhesion molecules modulate cell behavior in 3-dimensional culture. We hypothesized that cell adhesion, function and differentiation can be controlled by varying the amount of fibronectin in non-adhesive fiber matrices. The focus of this Master's Thesis is to investigate the development of nanofibrous protein cell supports with tunable adhesive properties. Our approach involved electrospinning mixtures of the globular protein bovine serum albumin (BSA) and fibronectin (FN) to mimic the elements of the architecture and biochemical composition of the ECM and support cell growth in a 3D scaffold.

A clinical study by Dror, Ziv, Makarov, Wolf, Admon and Zussman (2008) presented the first successful electrospun nanofibers made from BSA globular protein. Rich in cysteine BSA is involved in seventeen intramolecular disulfide bridges. Their procedure which was effective in the formation of strong nanofibers involved the opening of the disulphide bridges while the protein structure was unfolded to allow new structures with strong inter and intramolecular disulfide covalent bond to be formed.

With the application of these procedure as a driving force, we embraced a biomedical engineering approach to analyze the contribution of fibronectin polymerization on the varying physical and mechanical properties, adhesion strength and its support for  $\alpha_5\beta_1$  integrin binding and signaling through biochemical assays by analyzing the role that the cell adhesion protein plays when embedded in the electrospun BSA scaffolds, its advantageous properties with respect to focal adhesion, integrin binding and cell interaction with the ECM versus that of an electrospun fiber without the integration of fibronectin. Fibronectin is very important in the adhesion of cell because cells lack the presence of fibronectin on their own surfaces with can be associated with

cell migration and adhesion. In vitro, the extent of cell adhesion is related to the ability of cells to interact with fibronectin bound to matrix assembly sites and the ability of cell to or not to synthesize fibronectin. While some progress has been achieved in understanding components and structure of the ECM to date, there has been limited success in reconstructing the complex nature of the ECM to support tissue repair or regeneration. This Project is a first step towards understanding this complexity and developing biomimetic scaffolds for tissue engineering.

## 1.2 ELECTROSPINNING HISTORY

First discovered in 1902 by Marley and Cooley, electrospinning is an old polymer processing technique that involves the application of electric field to a polymer solution pumped at a constant rate through a syringe (Souheil Zekri et al. 2006). Electrospinning involves three simple steps used to obtain the desired fiber. They include a syringe pump to push the solution through a syringe forming a *Taylor cone* (pendant drop) on the tip, a voltage source that applies charge to the solution in the syringe metal needle thus generating the drawing forces, and a stationary grounded target to collect the produced fibers as shown in fig 1.1.

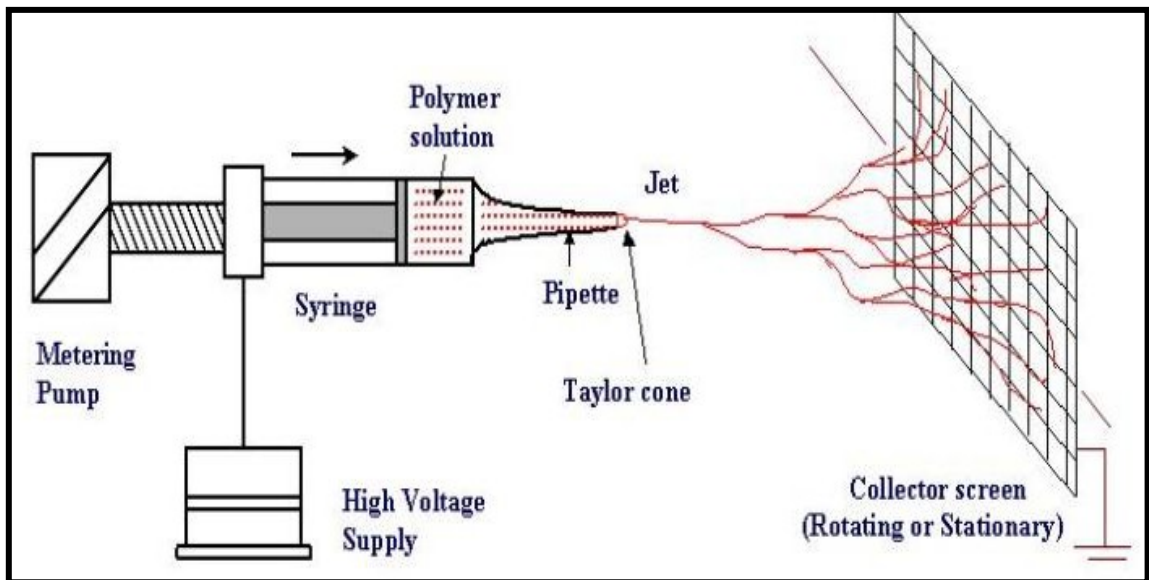


FIGURE 1.1: Schematic of the electrospinning setup. (Travis J. Sill and Horst A. Von Recum, 2008)

However, there are four main adjustable parameters that can influence the morphology of the electrospun structure which are the concentration of the solution, the applied voltage to the needle, working distance between the needle and the target and the

flow rate at which the polymer solution is being pumped out of the syringe (M. Bognitzki, T. Frese, J.H. Wendorff et al. 2000). The electrode from the voltage source is attached to the metal tip of the syringe needle and when turned on, a high charge of a certain polarity is injected. When the strength of the electric field is increased, the charges in the solution repulse each other and the opposite charges solution and grounded target starts to exert tensile forces on the solution which stretches the pendant drop that forms on the syringe metal tip thus elongating it (Travis J. Sill and Horst A. Von Recum 2008). With an additional increase in the electrical field, it reaches an equilibrium point in which solutions surface tension is balanced by electrostatic force forming the *Taylor cone* (Fig 2.1). When voltage is applied beyond the point of the formation of a *Taylor cone*, a fibrous jet is emitted from its tip known as cone-jet and accelerates towards the grounded target collecting plate (Travis J. Sill and Horst A. Von Recum 2008).

The morphology and diameter of the produced fibers can also vary based on the solution properties which include its nature, molecular weight of the polymer, concentration, volatility and conductivity of the solution (Table 1) (J.Doshi and D.H. Reneker 1995). Travel of the fibrous jet from the tip of the *Taylor cone* to the grounded target has brought about numerous explanations and in recent findings, Reneker conducted experiment to capture images of the emitted jet using a high-speed photography which captures 2000 frames per second (J.M. Deitzel, J.Kleinmeyer, D. Harris et al., 2001). If the fibers are still wet upon contact with the grounded target, they will join to and from junctions with other fibers to some degree. So by increasing the concentration of the polymer, we can eliminate the risk of producing wet fiber that would agglomerate with other fibers (J.M. Deitzel, J.Kleinmeyer, D. Harris et al., 2001).

After the jet was ejected from the tip, it became unstable bending back and forth increasing its vibrations to achieve a spiral path that in circumference as the diameter of the jet reduced along the path to the grounded target (Yarin AL, Koombhongse S. Reneker DH 2001). The instabilities of jet cause thinning and elongation as depicted in fig 1.2.

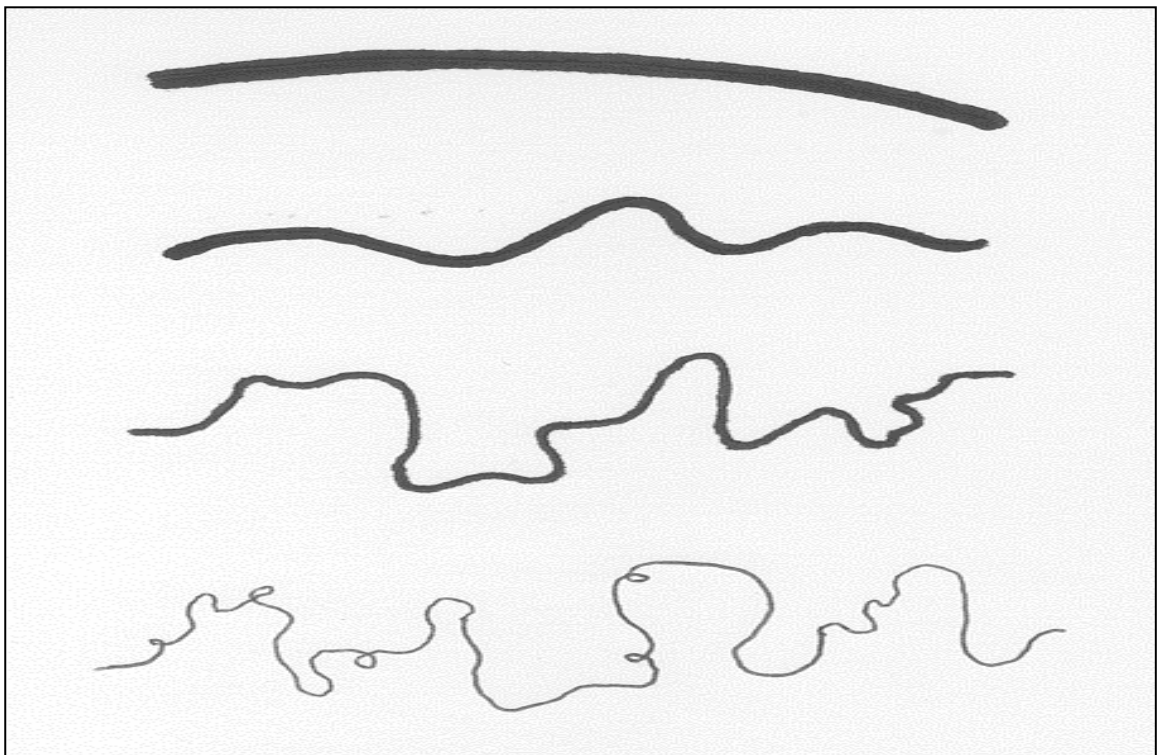


FIGURE 1.2: Diagrammatic representation of successive jet instabilities causing elongation and thinning. (Darell H. Reneker, and Alexander L. Yarin 2008)

Fig 1.3 shows the path of the electrospinning jet that contained three successive electrical bending instabilities (Darell H. Reneker, and Alexander L. Yarin 2008). The straight segment transformed into a three-dimensional coil which then transforms into to a smaller spiral until solidification of the jet occurs when the solvent evaporates between ejected from the jet and reaching the target (Hohman, M.M., Shin, M., Rutledge, G.,

Brenner, M.P., 2001). Four successive jet instabilities were observed in the experiments as depicted in figure 1.2 & 1.3 and after of the onset of this instability, all segment of the formed coil proceeded in an outward, downward manner which was categorized as not being random (Darell H. Reneker, and Alexander L. Yarin 2008).

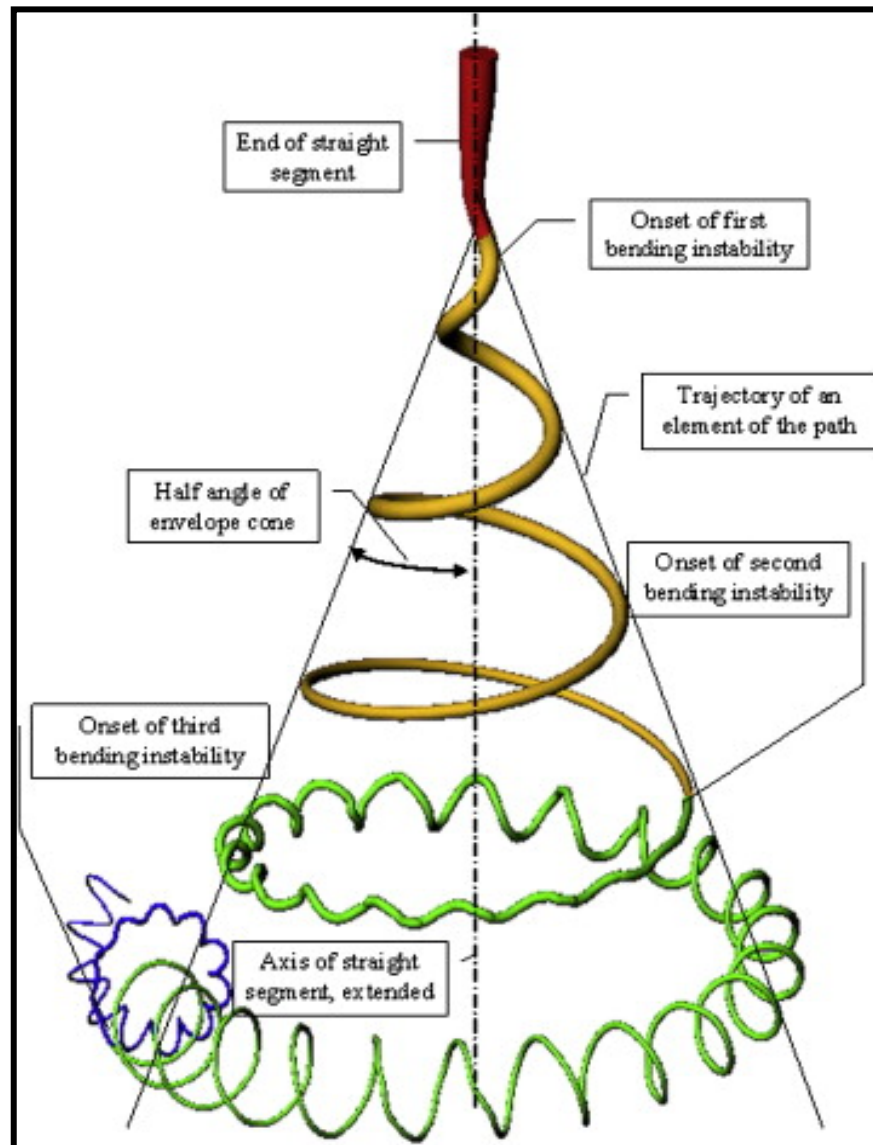


FIGURE 1.3: Diagram showing the instantaneous position of the path of an electrospinning jet that contained three successive electrical bending instabilities. (Darell H. Reneker, and Alexander L. Yarin 2008)

While significant research has been done on the electrospinning one fact remains clear that the state the electrospun fibers and mat produced are easily affected by variation in the solution concentration and the processing parameters. So to produce uniform fibers, both need to be optimized (J.M. Deitzel, J. Kleinmeyer, D. Harris et al., 2001). However, the characteristic of the polymer solution is the key to determining the fiber characteristics which include its diameter, elasticity, conductivity and tensile strength. In recent studies to understand the processing parameters, nanofibers with diameters ranging from 100-500nm were developed leading to a rapid rise in interest in the field of electrospinning because of its potential application in drug delivery process, tissue engineering field, filtration, protective clothing and so on (Travis J. Sill and Horst A. Von Recum. 2008).

### **1.3 PROCESSING PARAMETERS**

In addition to the polymer structure in the chosen solvent, several processing parameters control the properties of the electrospun fibers. These process parameters include the applied voltage, flow rate, distance between capillary and target, polymer concentration, conductivity of solution and volatility of solution. Manipulation and optimization of these parameters permits control over the production of fibers with varying diameter, pore size, scaffold surface topography and chemistry. So it is very important that the parameters are optimized to achieve an efficient electrospinning process.

### 1.3.1 Applied Voltage

This parameter and resulting strength of the electric field applied to the system controls the morphology and the diameter of the fiber produced which ranges from several microns to tens of nanometers (J.M. Deitzel, N.C. Beck Tan, J.D. Kleinmeyer et al., 1999). When more resistance but less force is applied the solution is drawn into a jet leading to thinner fibers. So the lesser the force, the thinner the fiber. In the investigation of the effect of voltage on the fiber formation of bead defects, Deitzel et al discovered that the number of beads defect increased (fig 1.4) in accordance to an increase in the failure to form jets from the solution. This failure was attributed to the fact that the rate at which the solution was pushed out from the metal tip was greater than that in which it was delivered to the tip. As seen in fig 1.5, when the applied voltage in increased, the volume of the pendant drop which is formed at the capillary tip reduces until the formation of *Taylor cone* at the tip. Thus by increasing the voltage applied, the fiber jet resulting in jet instability and is associated with bead defects as it is ejected from within the capillary (Hayati I, Bailey AI, Tadros TF 1987).

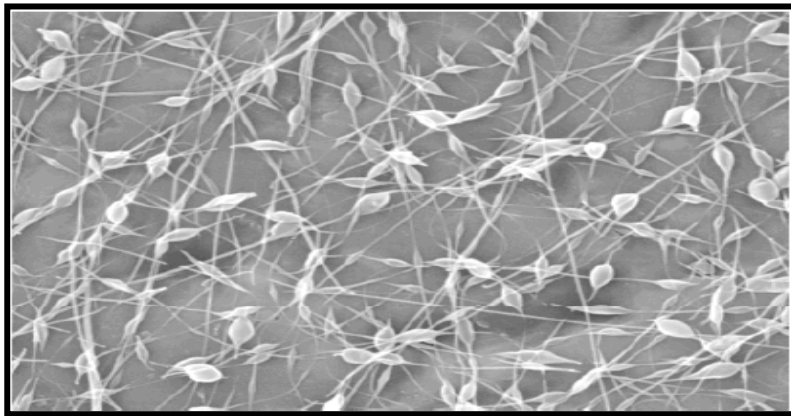


FIGURE 1.4: Beads created during electrospinning. (Hayati I, Bailey AI, Tadros TF, 1987)

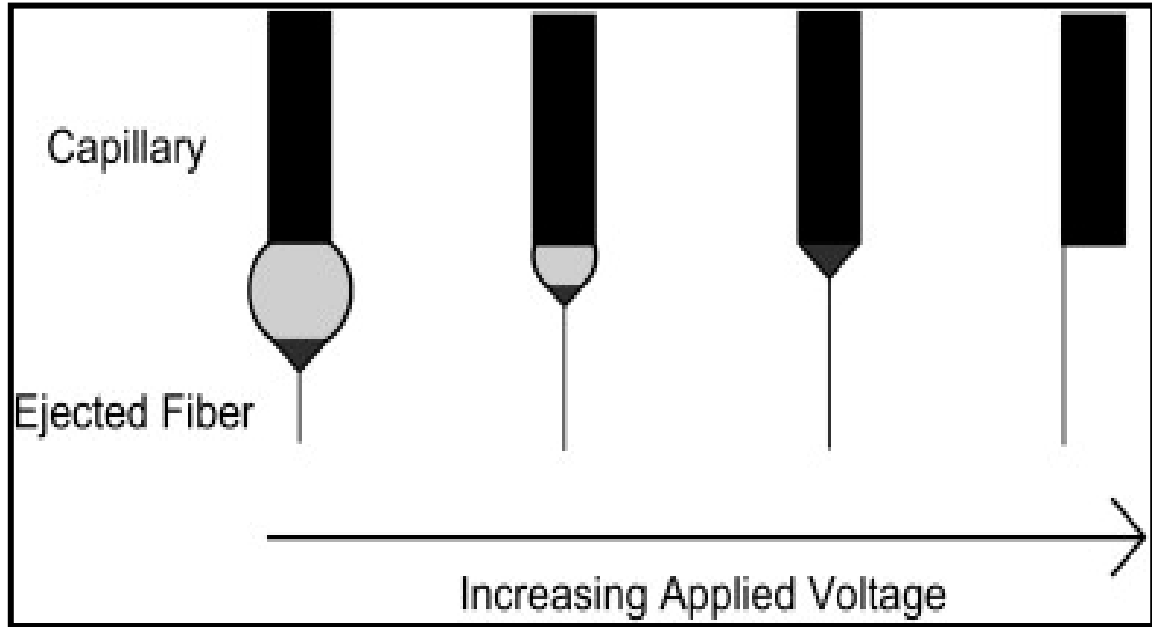


FIGURE 1.5: Effect of varying the applied voltage on the formation of the Taylor cone. (Hayati I, Bailey AI, Tadros TF, 1987.)

### 1.3.2 Flow Rate

Fiber morphology, porosity and diameter are also impacted by the flow rate of the system. Based on Fig 1.5 and the experiments on electrically driven jets conducted by Taylor who concluded that cone shape cannot be maintained if rate at which the solution was ejected from the metal tip as fiber jet was greater than that rate the solution flow through the capillary, the effect of flow rate on electrospun fibers made from polystyrene and tetrahydrofuran (THF) solution was carried out by Megelski et al (Taylor .G 1969). Megelski et al. demonstrated that the fiber diameter increase in accordance to increase to the flow rate and when the flow rate is high, there were noticeable bead defect which increased in availability as flow rate increases. This they described was due to the fact the fibers were unable to completely dry so on contact with the grounded target or collector

they were still wet join to and from junctions with other fibers and formed flattened or ribbon-like fibers (Megelski S. Stephens JS. Chase DB, Rabolt JF 2002). Fibers ejected at an optimal flow rate have a circular cross section.

### **1.3.3 Capillary to Target Distance**

The distance between the target and the tip of the capillary though plays a small role still influences the morphology of the fiber by about two magnitude orders (J.Doshi and D.H. Reneker 1995). This parameter can also determine whether electrospinning or electrospinning is achieved. As distance is increased, the diameter of the fiber decreases, and beads defects increase as distance is reduced which is due to the inability of the fiber to dry before reaching the target/collector (Megelski S. Stephens JS. Chase DB, Rabolt JF 2002).

### **1.3.4 Polymer Concentration**

The ability to achieve fiber formation is determined by the concentration of the polymer. The concentration of the polymer influences the two other important electrospinning parameters which are viscosity of the solution and its surface tension (Megelski S. Stephens JS. Chase DB, Rabolt JF 2002). The solution should not be overly concentrated or dilute but have a high enough concentration to form fiber jet. If the solution is too concentrated, the viscosity will be extremely high, the flow rate of the solution will not be able to be controlled and this will result in an inability of the formation of fiber of any diameter. So holding other parameter at a constant rate, for

fibers to be electrospun, the concentration of the polymer has to be at an optimum range (J.Doshi and D.H. Reneker 1995).

### **1.3.5 Conductivity of Solution**

Like the distance between the capillary and target, the solution conductivity can influence the size of the fiber in over two order magnitude. Thus, it plays a slightly less significant role than other electrospinning process parameters (Baumgarten P. 1971). Solutions that have low conductivity, has a lower charge carrying capacity than those of high conductivity. Thus in the presence of an electric field the fiber jet undergoes a greater tensile force thereby producing increasing fiber diameter (Hayati I, Bailey AI, Tadros TF 1987). Experiments conducted by Hayati et al concluded that solutions that have high conductivity levels when subjected to strong electric fields were very unstable resulting in a bending instability as seen in fig 1.3.

### **1.3.6 Volatility of Solution**

During the electrospinning process, a phase separation occurs between the capillary tip and the target/collector as the fiber jet is ejected from the tip to the target when the now solidified fibers are deposited reducing the effect of wet fibers. This phenomenon is greatly influenced by the volatility of the solvent which plays a vital role in fiber formation. A highly volatile solvent will increase the rate of evaporation of the gaseous or liquid phase, leaving only a solid phase (phase separation) which will in turn increase the surface area of the fibers (Megelski S. Stephens JS. Chase DB, Rabolt JF 2002).

## 1.4 INTEGRIN-MEDIATED CELL ADHESION

Cell adhesion to the extracellular matrix mediated by integrin receptors is vital to cell development and normal cell processes playing a critical role in cell communication, regulation and the development of tissues and in activation of signaling pathways that regulate cell differentiation, survival, cell cycle and development. The extracellular matrix is a complex structural network of structural, specialized proteins and proteoglycans that can interact with several of the surface receptors of the cell (De Arcangelis, A. and Georges-Labouesse, E., 2000).

Cell surface adhesion receptors known as integrin play a vital role during cell adhesion by mediating the attachment between cells to specific extracellular matrix proteins. Bound integrins cluster to form focal adhesion which strengthen adhesion and activate intracellular signaling pathways (Mu Gao and Klaus Schulten, 2004). Functional integrin receptors are  $\alpha\beta$  heterodimers (one  $\alpha$  subunit and one  $\beta$  subunit) which function as integrators or transmembrane linkers mediating actin cytoskeleton- ECM interaction. The subunits are bound together non-covalently so a particular ECM ligand maybe recognized by a specific subunit pair, and a variety of integrins can be made from a small number of subunits (Lotz, M.M., Budsal, C.A., Erickson, H.P., McClay, D.R., 1989).

Cell adhesion to other cells or to ECM is responsible for numerous metabolic and cellular activities such as formation of new blood vessels, wound healing, invasion and metastasis of tumor cells. So in order to be fully functional, cells must be able to bind to various molecules on the ECM or other cells (Anderson, J.M., Bonfield, T.L., and Ziats, N.P., 1990). Over the past years the understanding of integrin mediated adhesion has grown with regards to biochemical and signaling pathways and identification of adhesive

proteins and components which has been instrumental in understanding and deciphering mechanism that cell migration, adhesion and morphology and cellular functions.

## **1.5 PROJECT SIGNIFICANCE**

Our working hypothesis is that that cell adhesion, function and differentiation can be controlled by varying the amount of fibronectin in non-adhesive fiber matrices. The diameter, pore size, surface topography of the scaffold and chemistry of the electrospun scaffold has been engineered using electrospinning process and the contribution to adhesion has been quantified using a modified enzyme-linked immunosorbent assay (ELISA). First, a quantitative understanding of the contribution of optimized electrospinning parameters to achieve an efficient biocompatible and biodegradable matrix was established. Next the effect of processing and electrospinning the extracellular adhesion molecule, fibronectin, combined with the most abundant plasma protein in mammals, serum albumin, on cell adhesion was quantified. This work demonstrates the fabrication of a degradable protein nanofibers scaffold with tunable adhesive properties.

This research is innovative because it employs a biomedical engineering approach and manipulation to produce highly effective and strong nanofibers, analyze its structure –function relationship. It also applies integration of quantitative assays to analyze cell adhesion and manipulate it. The outcome establishes a framework for the analysis and production of electrospun scaffolds and studies of its structural, biochemical and mechanical components for cell processes and an understanding in the complexity in the development of biomimetic scaffolds for tissue engineering.

## **1.6 CONCLUSION AND CHAPTER OBJECTIVES**

This chapter provides detailed background information and describes the significance of electrospinning and cell adhesion. Chapter 2 will discuss the processing of bovine serum albumin fibers, measurement of the fiber diameter and document and discuss the results that were observed as the flow rate, polymer concentration, distance between capillary and target, voltage were controlled in order to obtain the low diameter continuous non-aligned fiber that is desired. In chapter 3, characterization of availability and bioactivity of fibronectin will be formulated from produced BSA, PBS and fibronectin films which will serve as experimental controls. Chapter 4 presents an in depth analysis of integrin binding and focal adhesion assembly on electrospun scaffold and films and ability to culture cells in order to study cell adhesion strengthening due to fibronectin availability. Finally, chapter 5 summarizes the conclusions gathered from the thesis research and offer suggestions for advanced study of cell adhesion strengthening.

**CHAPTER 2: ELECTROSPINNING DEGRADABLE NANOFIBROUS  
SCAFFOLDS FOR TISSUE ENGINEERING FROM GLOBULAR PROTEINS  
THAT REGULATE CELL ADHESION**

**2.1 INTRODUCTION**

Cells need a protective and stabilized environment for growth which is provided by the fibrous protein extracellular matrix (ECM). Over the last decade, due to the advantageous properties of fibrous proteins, research has been conducted using biocompatible and biodegradable natural polymers to develop biomimetic scaffolds for tissue engineering to mimic elements of the architecture and biochemical composition of the extracellular matrix. These synthetic or bioderived cell culture supports have been used to encourage cell growth and regulate its activities and for other biomedical applications (Mathews JA, Wnek GE, Simpson DG, Bowlin GL, 2002).

In order to achieve the mechanical properties of natural ECM fibers, artificial nanofibers with similar biocompatibility, strength, morphology surface to volume ratio is needed and this fabrication of this desired artificial nano-ultra fine polymeric fiber with the same natural quality is achieved through the process of electrospinning (Reneger, D. H, Yarin, A.L, Zussman, E. Xu, (2007). As a relatively simple method, it employs the manipulation of the electrospinning parameters such as distance from capillary to target,

concentration of polymer, flow rate, voltage to produce fibrous mats with controlled density (Shin, H. J, Lee, C.J, Cho, I.H, Kim, Y.J et al 2006).

It has also been found to be a simple and inexpensive method of producing nanofibers and for this reason, it has gained high and significant interest as an alternative way of producing nanofibers and scaffolds for biomedical applications and tissue engineering such as in drug or gene delivery, biosensor application, wound healing/dressing, electronics, fuel cell membrane and so on (Bhattacharai, S.R., Bhattacharai, N., Yi, H.K., Hwang, P.H., Kim, H.Y, 2004). However, it has been sometimes difficult to electrospin pure natural molecules as they have proven unstable for electrospinning because of the lack the essential viscoelastic properties and thus produce fibers whose mechanical properties are inferior to the natural fibers. In order to combat this setback, these molecules are often mixed with synthetic polymers to achieve the needed viscoelasticity before they are electrospun together (Bhattacharai, S.R., Bhattacharai, N., Yi, H.K., Hwang, P.H., Kim, and H.Y, 2004).

Several attempts have been made to electrospun silk fibroin fibers, as a single polymer and in addition to other polymers. However, the derived mechanical properties when compared to natural silkworm fiber produced inferior fibers. However the mechanical properties after the silk fibers were treated with methanol increased slightly which was attributed to the fact the methanol increased the formation of  $\beta$ -sheets (Chen, C. Cao, C. Ma, X. Tang, Y. Zhu, H.S 2006). Recently, production of a better preserved form of semi-crystalline structures of natural spider silk electrospun from hexafluoroisopropanol (HFIP) solution has been achieved in conjunction which the successful electrospinning of several fibrous proteins such as gelatin, collagen, fibrinogen

and elastin which though electrospinnable still produced fibers with inferior mechanical properties (Zarkoob, S. Eby, R. Reneker, D.H. Hudson, S.d., Ertly, D. Adams, W.W. 2004).

To produce scaffolds with excellent or good enough mechanical properties, chemical cross linking was attempted by Thomas et al in electrospinning keratin nanofibers which when separated into a smaller fraction with low cysteine availability and higher molecular weight and a larger fraction with a higher cysteine availability and lower molecular weight produced different mechanical properties. The larger fraction was only spinnable with the addition of another polymer which that of the smaller fraction could be spun in its occurring form (Thomas, E. Heine, E. Wollseifen, R. Cimpeanu, C. Moller, M 2005).

Here, this experiment presents the successful electrospinning of a stable nanofibers scaffold made of the globular protein bovine serum albumin (BSA) after optimization of all electrospinning parameters to achieve excellent physical properties which includes its fiber diameter and morphology. Bovine serum albumin (BSA) also known as was “Fraction V” and which has a human analogue (human serum albumin) was selected due to its stability, low cost, advantageous biochemical and biotechnological application such as a nonadhesive blocking agent, in immunoassays or as an enzymatic stabilizer, and more importantly due to the assumption that being one of the most abundant protein in the body, nanofibers electrospun from this globular protein would be biocompatible and not be rejected by the body by being considered less foreign (Peters, T 1995).

BSA is rich in cysteine which is involved in seventeen intramolecular disulfide bridges, the produced BSA nanofibers were achieved from reformed structures with strong disulfide covalent bonds produced from opening of the intramolecular disulfide bridges while unfolding the protein. The main challenge encountered involved not only being able to transform the BSA protein from its low viscous state into a solution that would be spinnable with strong intermolecular disulfide bridges but also being able to control the effect each electrospinning parameter would create on the production of a continuously, ribbon-like, nano- fiber if it is not optimized and also characterize how the morphology and diameter of the fiber produced can be affected by the parameters (Yael Dror, Tamar Ziv, Vadim Makarov, Hila Wolf, Arie Admon and Eyal Zussman 2008).

## **2.2 MATERIALS AND METHODS**

### **2.2.1 Materials and Solutions**

Bovine Serum Albumin (BSA) (Fraction V) of molecular weight  $67 \times 10^3$  Da was purchased from Fischer Scientific and to avoid any issues stemming from molecular heterogeneity, all experiments were performed with the same BSA sample and used without further purification. 2, 2, 2-trifluoroethanol (TFE, MW 100.04g/mol) and 99%  $\beta$ -mercaptoethanol (MW 78.13g/mol, 1.110g/ml density) were purchased from Sigma Aldrich. The corresponding volume of TFE was determined using the density of TFE at 20°C of 1.391g/ml.

TABLE 2.1: Chemical properties of materials

MATERIALS	COMPOSITION	
	Molecular Weight	Density
Albumin Bovine (BSA)	67 X 10 <sup>3</sup> Da	
2,2,2 Trifluoroethanol	100.04g/mol (C <sub>2</sub> H <sub>3</sub> F <sub>3</sub> O)	1.373 g/mol @ 25C 1.391 g/mol @ 20C
β-Mercaptoethanol (99%)	78.13 g/mol (C <sub>2</sub> H <sub>6</sub> O <sub>5</sub> )	1.110g/mol

### 2.2.2 Electrospinning

The BSA solutions were electrospun from a Becton Dickinson (B-D) tuberculin slip tip latex free 1ml syringe with an 18G x1/2" SS/needle. The flow rates were  $Q = 0.25$  ml/hr, 0.5 ml/hr and 1.0 ml/hr. A copper electrode supplying voltage was attached to the syringe needle and the BSA solution was spun on a onto a electrically grounded aluminum foil covered target plate (2" x 2"), 9x9 mm size #1 thickness cover-glasses were glued to the front face of the target as seen in Fig 2.1. The distance from the tip of the needle (capillary) to the target plate with cover slips were  $D = 12\text{cm}$ ,  $15\text{cm}$  and  $20\text{cm}$ . All experiments were performed at room temperature (24°C) and the resulting samples were stored in a dessicator.

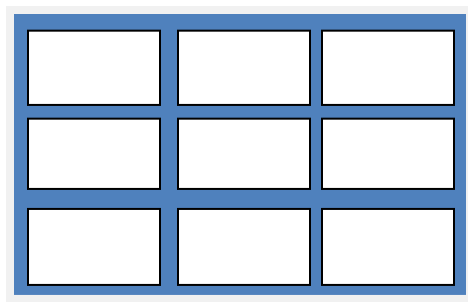


FIGURE 2.1: Aluminum foil covered target plate (blue) with cover slips (white) to collect electrospun fibers.

### 2.3 EXPERIMENTAL OVERVIEW

Bovine serum albumin (BSA) solutions with differing concentrations were prepared in a mixture trifluoroethanol and water (TFE/H<sub>2</sub>O 9:1 ratio) with and without the addition of  $\beta$ -mercaptoethanol which served as a protein structure modifier and fibronectin for cell adhesion purposes. A colorless liquid with an ethanol-like odor, TFE has been known to induce structural changes of proteins by interacting with the polypeptide chain, favoring local interactions and weakening nonlocal interactions and disrupting the proteins tertiary structure (Thomas PD, Dill KA. 1993). However, different conformational states are produced in accordance with different level of TFE concentration. At high TFE concentration, the protein tertiary conformation with regards to the hydrophobic interaction is disrupted and so is the structure of H<sub>2</sub>O. This is because in the presence of TFE, proteins tend to become more helical (open-helical structure) thus strengthening the intramolecular hydrogen bonds in the secondary structures which the tertiary proteins structures unfold causing a weak interaction between the segments of the structural helix with the solvent being able to interact with the exposed hydrophobic segments (Thomas PD, Dill KA. 1993).

With this theory as a backbone, we used a higher concentration of TFE which we hypothesized would create an open-helical structure protein which will enhance the ability to electrospin the BSA. Though the high concentration of TFE allowed the BSA solution to be more spinnable, it was very unstable forming no fiber or highly fragmented fiber (higher BSA concentration) as can be seen in *fig 2.3*. This resulting discovery of the TFE's inability to fully unfold the protein structure and allow protein-protein interactions which can be attributed to the globular structure (Thomas PD, Dill KA. 1993).

However, with the addition of  $\beta$ -mercaptoethanol ( $\beta$ -ME), a chemical compound used to reduce disulphide bonds, further denaturing and expansion of the protein occurred and the spinning process was extremely improved which in turn improved the mechanical properties and tensile properties of the produced fibers and their morphology. This can be attributed to the fact that  $\beta$ -ME was able to increasingly open up the protein helical structure and the intramolecular disulphide bridges (Thomas PD, Dill KA. 1993).

To analyze the effect of the key process parameters, electrospinning of the nanofibers were conducted under different conditions which included concentration, flow rate, capillary-target distance (C-TD), applied voltage, and temperature. Different concentrations (10-20 wt %) of BSA was prepared in 9:1 weight ratio of TFE/H<sub>2</sub>O, 10 equiv/bond  $\beta$ -mercaptoethanol and fibronectin (0, 0.1, 1 and 10  $\mu$ g/ml) that were electrospun at different capillary-target distance (12 – 20cm) and flow rates (0.25 – 1 ml/hr).

### 2.3.1 Effect of Solvent on Fiber Morphology

The first experiment began with electrospinning a solution composing of 10% BSA, 9:1 TFE/ H<sub>2</sub>O, 0g of fibronectin and no β-mercaptoethanol. The original recipe for the solution and process parameters and its calculations is summarized in table 3.1 and figure 3.2 below.

TABLE 2.2: Original process parameter

Parameter	Values
Distance	12cm
Voltage	13kv
Rate	0.25ml/hr
Volume	0.1ml

<p><b><u>9: 1 TFE/ H<sub>2</sub>O</u></b>            Total volume needed = 5ml  <math>\frac{9}{10} \times 5 = 4.5\text{ml TFE}</math>     <math>\frac{1}{10} \times 5 = 0.5\text{ml H}_2\text{O}</math></p>	<p><b><u>10% BSA</u></b>  <math>\frac{10}{100} \times 5\text{ml} = 0.5 \text{ g BSA}</math></p>					
<p><b><u>10equiv/β-ME</u></b></p> <table border="1" style="margin-left: auto; margin-right: auto;"> <tbody> <tr> <td style="padding: 2px;"><math>\frac{0.5\text{g BSA}}{67 \times 10^3\text{g}}</math></td> <td style="padding: 2px;"><math>\frac{1 \text{ mol BSA}}{1 \text{ mol BSA}}</math></td> <td style="padding: 2px;"><math>\frac{170 \text{ mol } \beta\text{-ME}}{1 \text{ mol BSA}}</math></td> <td style="padding: 2px;"><math>\frac{78.9\text{g } \beta\text{-ME}}{1 \text{ mol } \beta\text{-ME}}</math></td> <td style="padding: 2px;"><math>\frac{1\text{ml}}{1.11\text{g } \beta\text{-ME}}</math></td> </tr> </tbody> </table> <p>=89.5μl β-ME</p>		$\frac{0.5\text{g BSA}}{67 \times 10^3\text{g}}$	$\frac{1 \text{ mol BSA}}{1 \text{ mol BSA}}$	$\frac{170 \text{ mol } \beta\text{-ME}}{1 \text{ mol BSA}}$	$\frac{78.9\text{g } \beta\text{-ME}}{1 \text{ mol } \beta\text{-ME}}$	$\frac{1\text{ml}}{1.11\text{g } \beta\text{-ME}}$
$\frac{0.5\text{g BSA}}{67 \times 10^3\text{g}}$	$\frac{1 \text{ mol BSA}}{1 \text{ mol BSA}}$	$\frac{170 \text{ mol } \beta\text{-ME}}{1 \text{ mol BSA}}$	$\frac{78.9\text{g } \beta\text{-ME}}{1 \text{ mol } \beta\text{-ME}}$	$\frac{1\text{ml}}{1.11\text{g } \beta\text{-ME}}$		

FIGURE 2.2: Mathematical calculation of electrospun materials

The type of solvent chosen is very important in obtaining a stable scaffold. In this study, TFE was initially chosen because it was a good solvent for BSA polymer, it had been known to induce structural changes of proteins and create a more open helical protein structure which will allow for electrospinning. However, the images of the resulting fibers indicated that the electrospinning process was highly unstable producing fibers that has uneven diameter, short and non-continuous as can be seen in fig 2.3a. However, when  $\beta$ -mercaptoethanol was added, the electrospinning process became relatively stable producing a continuous fiber with smooth surface as can be seen in fig 2.3b. As mentioned in the previous section  $\beta$ -mercaptoethanol ( $\beta$ -ME), a chemical compound that reduces disulphide bonds, and enhances further denaturing and expansion of the protein. These characteristics improved the electrospinning stability by opening up the protein helical structure and the intramolecular disulphide bridges enabling new inter and intramolecular bonds to be reformed.

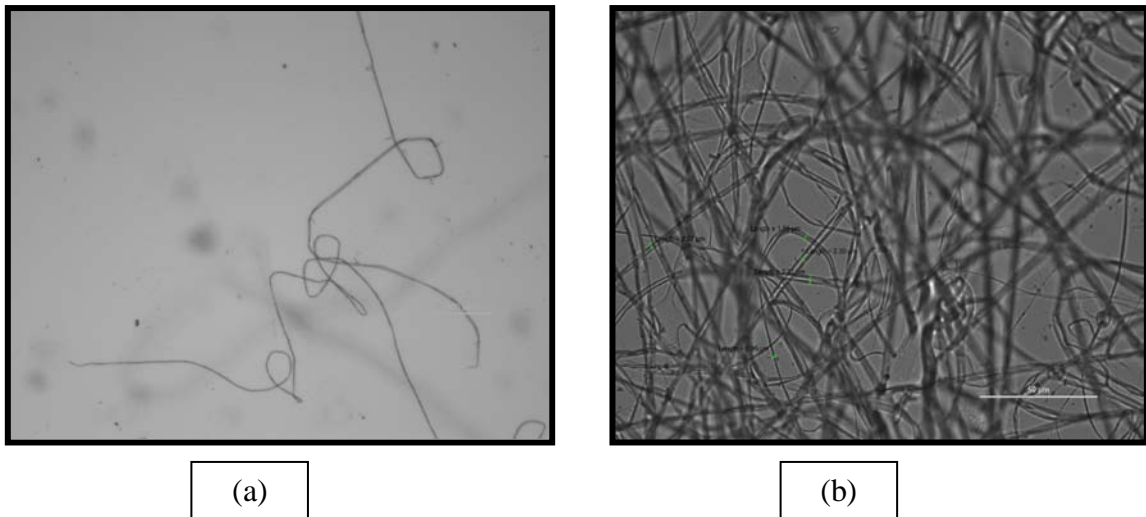


FIGURE 2.3: Comparison of BSA fibers with and without addition of  $\beta$ -mercaptoethanol (a) without (b) with (10x)

### 2.3.2 Effect of Concentration

BSA concentrations of 10%, 12%, 15% were used to investigate the effect of polymer concentration on the fiber morphology. The applied voltage at a value of 14kv and the distance from the capillary to the target (15cm) were kept constant. The result showed that increasing the concentration while keeping other parameters constant significantly increases the diameter of the fiber. However, the solution with high concentration (20%) was very difficult to spin, most likely due to effect of surface tension on the ability of the solution to be ejected from the syringe needle. A microscopic image of the fibers are given in *fig 2.4*, the results of the concentration to diameter analysis of the electrospun BSA mats are given in *table 2.3* are graphically represented in *figure 2.5*.

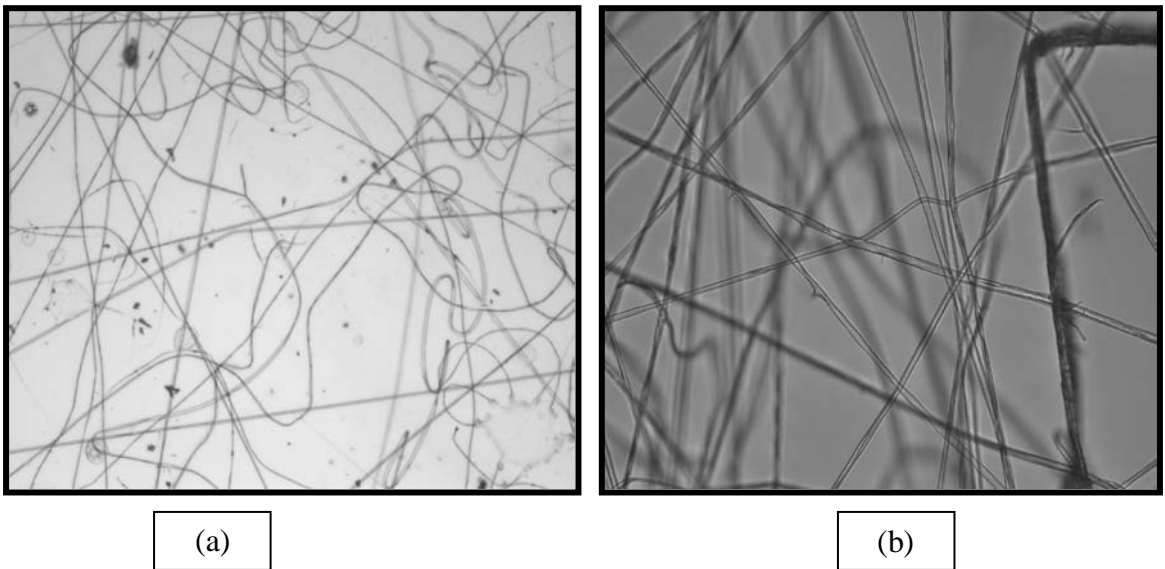


FIGURE 2.4 Effect of BSA concentration on fiber diameter (a) 10% BSA, (b) 15% BSA (10x)

TABLE 2.3: Fiber diameter measurement analysis to illustrate the relationship between concentration of electrospun BSA and fiber dimensions.

BSA Conc (%)	Fiber Diameter ( $\mu\text{m}$ )						
	Diameter ranges ( $\mu\text{m}$ )					Mean	Standard Dev.
	1	2	3	4	5		
10	2.06	1.99	1.89	1.86	1.84	1.92	0.08
12	2.33	2.27	2.12	2.01	2.00	2.15	0.13
15	2.73	2.44	2.42	2.24	2.11	2.39	0.21

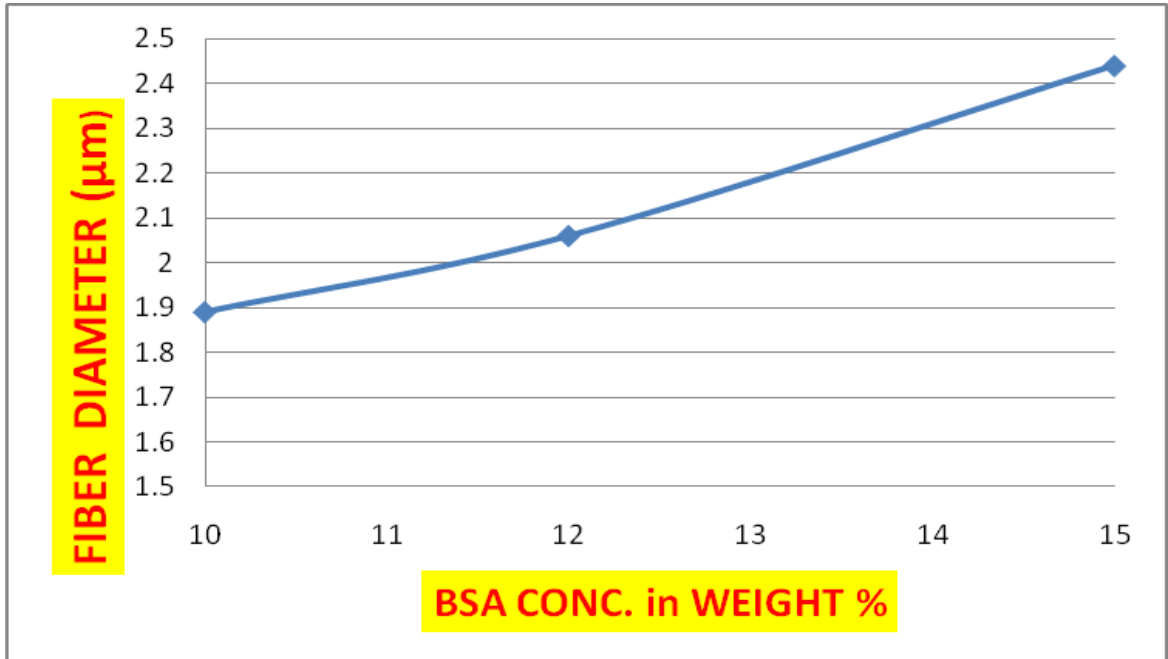


FIGURE 2.5: Fiber diameter measurement analysis to illustrate the relationship between concentration of electrospun BSA and fiber dimensions.

### 2.3.3 Effect of Flow Rate

To investigate the effect of flow rate on the fiber morphology of BSA fibers, 10 weight %, 12weight % and 15weight % of BSA solutions were selected for each weight percent to be investigated at a constant voltage of 14kv and at a rate of 0.5ml/hr with differing distance of 12cm, 15cm and 20cm. The trend to show the effect of rate results is depicted in *fig 2.6* which shows a positive correlation between solution flow and electrospun BSA fiber diameter which would indicate that as the rate increases, the fiber diameter increases. This is most likely due to the fact that more force applied to push the solution out of the syringe and less resistance by the voltage to draw the fiber jet out. With the fiber forced out instead of drawn out and are not completely dry on contact with the grounded target thus forming semi-flattened or flattened fibers depending on how high the flow rate is. The lesser the flow rate, the smaller the fiber diameter.

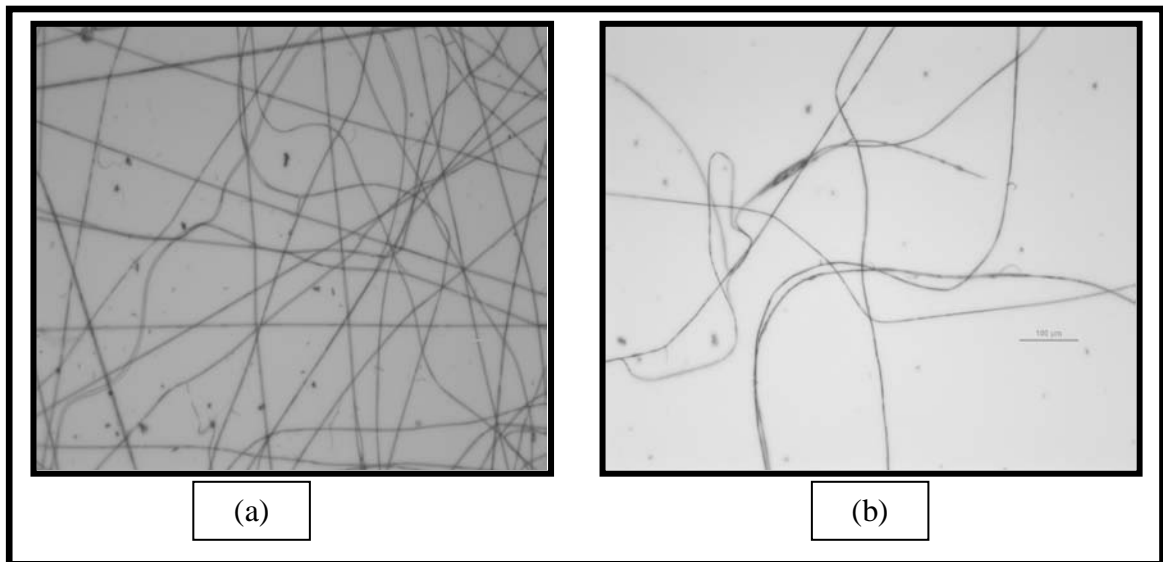


FIGURE 2.6: Effect of flow rate on fiber diameter at 12% concentration, 12 cm (a) 0.25ml/hr flow rate (b) 1.0ml/hr (10x)

TABLE 2.4: Fiber diameter measurement analysis to illustrate the relationship between flow rate of electrospun BSA and fiber dimensions.

Flow rate (ml/hr)	Fiber Diameter ( $\mu\text{m}$ )						
	Diameter ranges ( $\mu\text{m}$ )					Mean	Standard Dev.
	1	2	3	4	5		
0.25	2.28	2.30	2.36	2.50	2.53	2.39	0.10
0.5	2.98	2.95	3.19	3.55	3.59	3.23	0.29
1.0	3.81	3.86	3.89	4.00	4.11	3.93	0.11

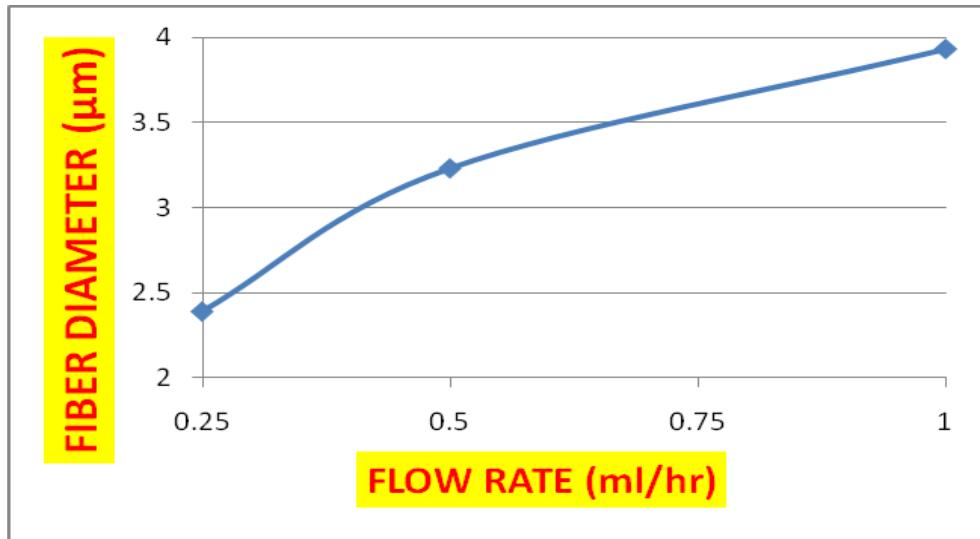


FIGURE 2.7: Summary of the effect of flow rate to fiber diameter

### 2.3.4 Effect of C-TD Distance

To investigate the effect of collecting distance on the fiber morphology of BSA fibers, 10 weight%, 12 weight% and 15weight% of BSA solution was selected at a constant voltage of 14kv and at a rate of 0.5ml/hr and at varying distance of 12cm, 15cm

and 20cm. It can be seen that by increasing the capillary to target distance (C-TD), the average fiber diameter decreases. This result was true for all the fibers spun at different concentration, electric potential and flow rate. *Fig 2.8* illustrates the effect of collecting distance on the fiber diameter at 12% BSA over a fixed applied voltage of 14kv and a rate of 0.25ml/hr. It can be observed that by increasing the capillary target distance, the fiber diameter decreases. Trends that were observed at higher concentrations but at lower concentration (10% BSA) *Fig 2.9*, blobs were observed which should not be mistaking as beads.

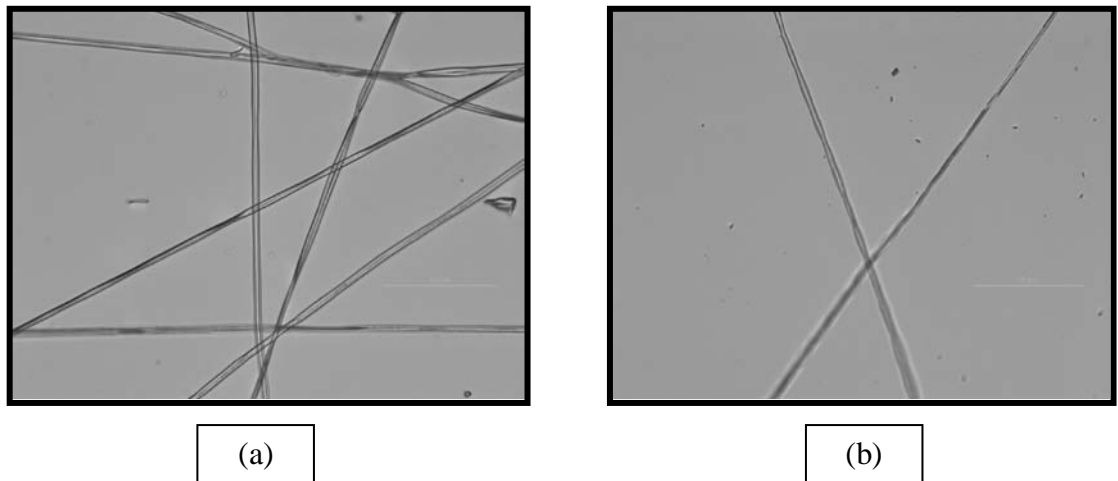


FIGURE 2.8: Effect of collecting distance on the fiber diameter at 12% BSA (a) 12 cm (b) 20cm (40x).

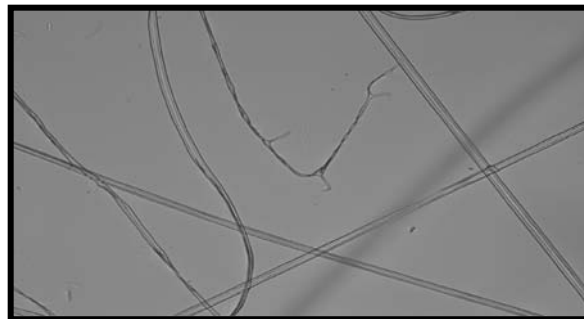


FIGURE 2.9: Effect of collecting distance on lower concentration BSA (10%) showing blobs (40x).

TABLE 2.5: Electrospun 12% BSA fiber with differing distance and mat characteristics

Distance (cm)	Fiber Diameter (nm)						
	Diameter ranges ( $\mu\text{m}$ )					Mean	Standard Dev.
	1	2	3	4	5		
12	2.99	2.30	2.36	2.50	2.53	2.39	0.10
15	2.33	2.27	2.12	2.01	2.00	2.15	0.13
20	1.93	1.54	1.41	1.37	1.28	1.51	0.23

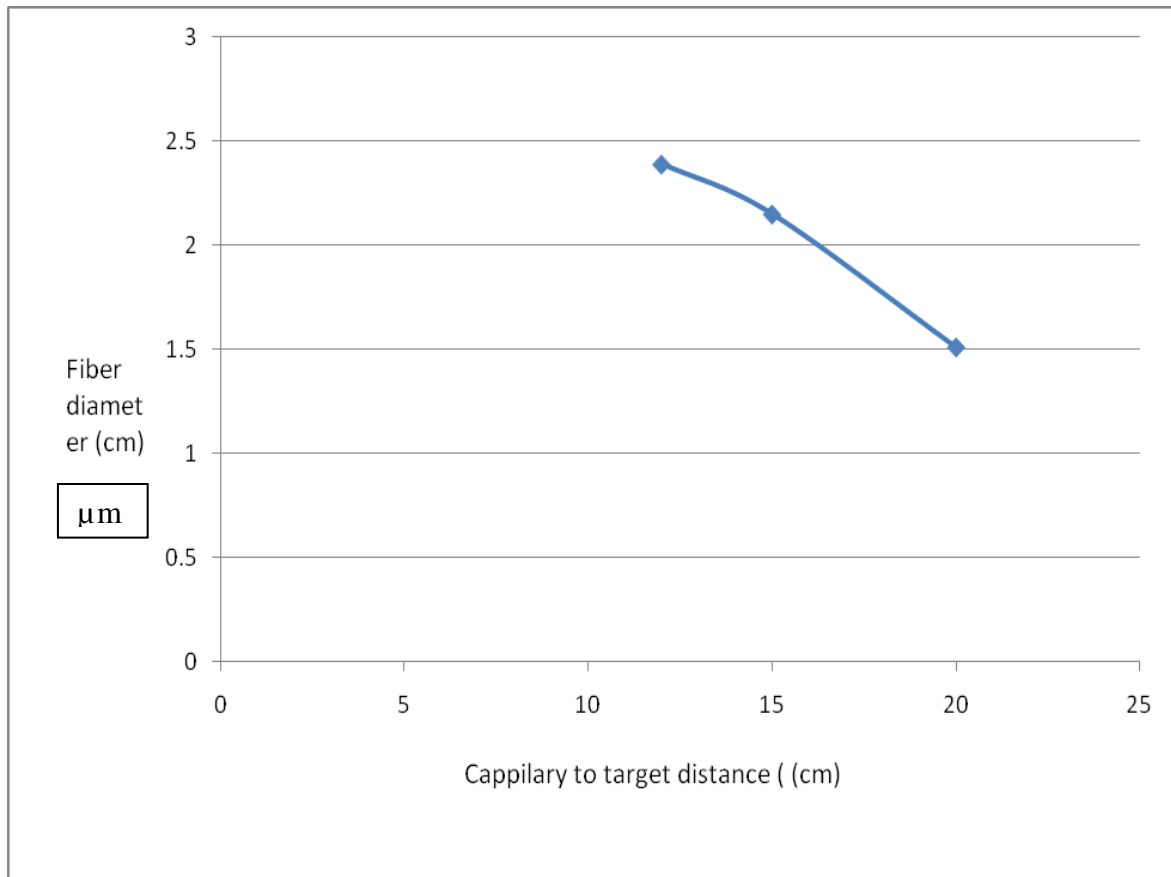


FIGURE 2.10: Summary of the effect of capillary to target distance

### **2.3.5 Effect of Applied Voltage**

High applied voltage are expected to result in increased electrostatic forces and increased drawing stress on the fiber jet which should in turn produce fibers with reduced diameters. This was the case in this study as the fibers formed had lower diameters owing the significant increase in the applied voltage. Furthermore, we were still able to obtain a low enough potential that was just enough to exceed the limit to form the *Taylor cone* and produce a fiber jet with no bending instabilities.

### **2.3.6 Effect of Temperature**

Temperature was not included as one of the processing parameter because it has not been considered as having an adverse effect on the fiber morphology. However in this study, temperature was shown to only have an effect on the reaction time of the BSA with the reducing agent. The reaction time at room temperature was faster than at a cooler temperature. This factor affects the morphology of the fiber producing a false negative ideology that better fibers can be produced over an increased period of time such as 24, 48 and 72 hrs. An experiment was conducted using 12% and 15% BSA concentration stored under room a temperature ( $\sim 23^{\circ}\text{C}$ ) and  $4^{\circ}\text{C}$  as seen in *table 2.6*.

TABLE 2.6: Temperature (°C ) vs. reaction time (hr)

Temperature	Reaction Time (hrs)
Room temp vs. 4°C	24
	48
	72

At room temperature, both 12% and 15% BSA solution reacted at the same rate over a 24hr period and exceeding this time limit did not affect electrospinning process thus producing stable fibers. So after 24hr, time was not a factor in affecting the stability of the BSA solution for electrospinning. However, after 24hrs, the stability of both concentrations for electrospinning was totally different. The reaction rate under the cooler temperature was very slow for both concentration but slower for the lower concentration. So when electrospun, the produced fibers differ in morphology as reaction time for the solution progressed from 24 hrs to 48 hrs to 72 hrs thus giving providing a false negative ideology that better fibers can be produced over an increased period of time.

With these results, it can be concluded that storage at room temperature provides a better environment for electrospinning the BSA solution because extended reaction time are not required to produce stable fibers with reproducible properties. At room temperature reaction, the morphology of the resulting fiber is not dependent on time after 24 hours. Thus, no matter how long various BSA concentrations are stored for, their

reaction time would be similar and quantitative analysis of fiber morphology would not be affected.

## **2.4 EQUIPMENTS**

A high voltage AC to DC converter power supply permitting voltage adjustment in a range of 0-30kV was used as integral part of the electrospinning. A syringe pump was used to maintain the constant volume flow rate as the polymer solution is being pumped through the syringe. An inverted microscope (Nikon, Ti-U) with oil condenser lens (T-C High NA, object distance of 1.92mm, magnification ranging from 10-100x), HG precentered fiber illuminator (Nikon, HGFI), differential interference contrast (DIC), fluorescence filters (FITC, emission band 515- 555nm and an excitation band of 465-490nm) and intensilight (Nikon, C-HGFI) was used to obtain the fiber images. A spectrophotometer (Synergy 2) was used to measure fibronectin intensity as a function of the light source wavelength at 405nm absorbance.

## **2.5 CONCLUSION**

Electrospinning of BSA into a fibrous mat is an exceptional achievement because it is a globular protein. In this experimental study, our aim was to demonstrate the feasibility of electrospinning BSA globular protein, to quantify the electrospinning process parameter and demonstrate the capability of adjusting the physical properties of the scaffold by changing the concentration, rate, distance and voltage based on the type of polymer used. Table 2.7 summarizes the effect of differing processing parameter.

In conclusion, fibers made from BSA dissolved in TFE/H<sub>2</sub>O and  $\beta$ -ME have been successfully electrospun with controllable and morphology. This achievement can be attributed to the protein conformation being manipulated by reducing the S-S disulfide bonds allowing for intermolecular entanglement and bonding under the conditions of combined denaturing TFE environment and reducing  $\beta$ -ME environment.

The optimal parameters as listed in *table 2.7* to be used for further study will be 12% at a distance of 15cm and at a rate of 0.25ml/hr. Using this baseline parameter set, various concentration of the adhesive protein fibronectin will be incorporated into BSA solution and, electrospun to produce adhesion regulating protein mats. The fibronectin availability and bioactivity in the electrospun scaffold will be characterized as detailed in chapter 3 and in also in the investigation of cell adhesion and focal adhesion assembly on electrospun BSA scaffolds as detailed in chapter 4. In the future these fibrous mats with tunable architecture and adhesive properties will serve as scaffolds in tissue engineering applications.

TABLE 2.7: Composition of FN incorporated into optimized parameter from electrospun fibers

<b>Composition of Optimized parameter for further study</b>	<b>Conc. of Incorporated Fibronectin (<math>\mu\text{g/ml}</math>)</b>
12% , 15cm, 0.25 mi/hr	0.1
	1.0
	10

TABLE 2.8: Summary of the effect of the different processing parameters

Parameter	Effect on fiber morphology
Applied voltage ↑	Fiber diameter initially ↓ then ↑
Flow rate ↑	Fiber diameter ↑ (if flow rate is too high, beads morphologies occur)
Distance between capillary and collector ↑	Fiber diameter ↓ (beaded morphologies occur if the distance is too short)
Polymer concentration (viscosity) ↑	Fiber diameter ↑ within an optimal range
Solution conductivity ↑	Fiber diameter ↓
Solution volatility ↑	Fiber surface area ↑

**CHAPTER 3: CHARACTERIZATION OF FIBRONECTIN AVAILABILITY  
AND BIOACTIVITY UNDER THE CONDITIONS OF ELECTROSPUN  
SCAFFOLD FABRICATION**

**3.1 FIBRONECTIN**

Cells are connected together in tissues through a protein network known as the extracellular matrix which also guides the movement of cells during wound healing, cell development and sends signals to cells. One of the essential components of the extracellular matrix is fibronectin (De Arcangelis, A. and Georges-Labouesse, E., 2000). Fibronectin (FN) is a multifunctional extracellular matrix glycoprotein that exists as a dimer composed of two identical polypeptides disulphide bound with a molecular weight of ~ 400kDa (per dimer) FN assembles into fibrils that binds to membrane receptor protein known as integrins and attaches cell to the ECM (Potts JR and Campbell ID. 1994).

Fibronectin adhesion has numerous functions that include cell morphology, homeostasis, cytoskeleton organization and so on and various studies has shown that cell adhesion, spreading and migration can be enhanced by fibronectin both in cell culture experiments and in vivo (Potts JR and Campbell ID, 1994). Assembled into the extracellular matrix is cellular fibronectin which is similar to insoluble plasma globulin in structure and also in it antigenic properties allowing cross reaction with polyclonal

antibodies. Production of fibronectin is very common by mesenchymal and epithelial cell such as intestinal epithelial cells, hepatocytes, macrophages and Schwann cells (Potts JR and Campbell ID, 1996).

Type III fibronectin module does not contain any disulfide bridges allowing it to unfold with any application of force. However, intra-chain disulfide bridges are available in type I and type II modules to provide them with stability. (Baron M, Main AL, Driscoll P.C., Mardon H.J., Boyd J., Campbell ID, 1992).

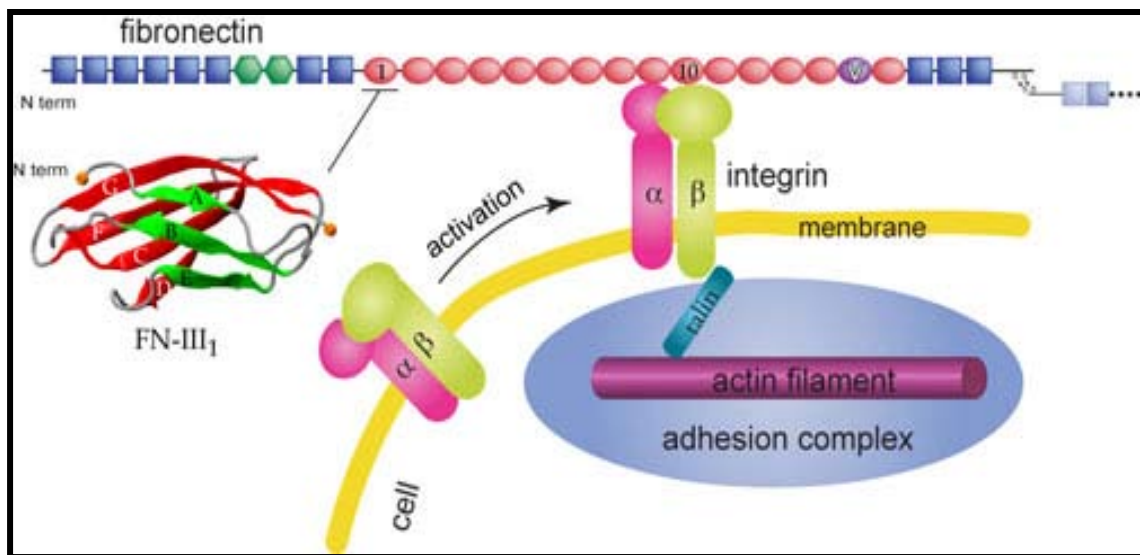


FIGURE 3.1: Fibronectin bound to integrin at the cell surface

## 3.2 MATERIAL AND METHODS

### 3.2.1 Statistical Analysis of Variance (ANOVA)

A one-way analysis of variance was used to compare the means of three samples from each population (0FN, 1FN, 10FN).

### **3.2.2 Antibodies**

Polyclonal rabbit anti-fibronectin antibodies was purchased from Sigma Aldrich while polyclonal goat anti-rabbit IgG antibody used for in indirect measurement and indication of the presence of fibronectin were purchased from invitrogen. Monoclonal mouse anti-human fibronectin clone HFN7.1-supernatant antibody was purchased from developmental studies hybridoma bank and monoclonal goat anti-mouse IgG antibodies conjugated to alkaline phosphatase as 2<sup>o</sup> antibody was purchased from Jackson immuno research.

### **3.2.3 Surface Coating with BSA and Fibronectin**

Glass cover slips (9x9 mm size #1 thickness) were cleaned in 70% ethanol, and dried. Per cover slip, 100  $\mu$ L of 12% BSA solution concentration (in TFE/H<sub>2</sub>O or PBS solvent), TFE/H<sub>2</sub>O and PBS solvent of fibronectin or no fibronectin was deposited on it. After deposition, the glass cover slips were incubated with 1% BSA solution (1gram BSA dissolved in 100ml of PBS solution) as a blocking buffer for 1 hour to block nonspecific adhesion to glass. Adhesion was not found on glass cover slips coated with the blocking buffer.

### **3.2.4 Elisa**

After blocking, the samples on the glass cover slips were incubated with either polyclonal antibodies (PAbs) or monoclonal antibodies, followed by secondary antibodies conjugated to alkaline phosphatase and then substrate buffer (0.2M Tris Buffer + 5mM MgCl<sub>2</sub> in dH<sub>2</sub>O + p-Nitrophenyl phosphate tablets) for 30min and the reaction

stopped by the addition of 50 $\mu$ l of 3M NaOH per 200 $\mu$ l of reaction mixture. In between each step the samples were washed with DPBS (+ calcium chloride, + magnesium chloride) and the microtiter plates were put into an absorbance spectrophotometer plate reader (Biotek Synergy 2 SLFA) with a filter set (Excitation 360/40, 485/20, 530/20 and Emission 460/40, 528/20, 590/35). This instrument allowed for a light source to illuminate the sample using a specific wavelength (405nm) and as a result of this illumination, the sample absorbs light. A light detector measures how much of the initial light is transmitted through the sample. The amount of light absorbed relates to the concentration of the fibronectin adsorbed into the sample.

### **3.3 RESULTS**

#### **3.3.1 Fibronectin Analysis**

To analyze the amount of fibronectin that was available, in the fibers by measuring alkaline phosphatase activity using the ELISA method.

#### **3.3.2 (TRIAL 1) Staining for Fibronectin in Electrospun Fibers**

BSA electrospun fibers with differing amount of fibronectin (0 $\mu$ g/ml, 1 $\mu$ g/ml & 10 $\mu$ g/ml) were deposited on a cover glass and stained for fibronectin availability with polyclonal antibodies using the method of ELISA. *Fig 3.2* shows the arrangement of the fibers in the plate which also included a control sample which did not include the electrospun fiber but just the substrate buffer.

### 3.3.2.1 (TRIAL 1) Results

The results obtained from the spectrometer reading contradicted our expected results. Since we electrospun several fibers with varying amount of FN, we expected that staining for the availability of fibronectin on the fibers will produce a data showing the concentration of FN adsorbed into the sample increase according to the initial amount of fibronectin that was available. The light transmits a yellow color which indicates the intensity of the adsorbed fibronectin.

However, the data did not support the amount of fibronectin available in the original sample. Samples with the larger amount of FN emitted light was recorded to be about the same or even lower than samples that had lower or no amount of FN. It also showed all samples from the BSA fibers with no FN to have the same result as the BSA fibers with 1ug/ml FN.

TABLE 3.1: Trial 1 FN absorbance data

SAMPLE	BSA fibers + 0ug/ml FN	BSA fibers + 1ug/ml FN	BSA fibers + 10 ug/ml FN
1	0.110	0.109	0.107
2	0.109	0.11	0.112
<b><u>MEAN</u></b>	<b><u>0.1095</u></b>	<b><u>0.1095</u></b>	<b><u>0.1095</u></b>

The results of this preliminary experiment were inconclusive because the results showed that all the fiber scaffolds had no significant difference in their fluorescence intensity even though there was supposed to be based on the fact that different amount of fibronectin was incorporated to the BSA fibers. Our expected results was that by increasing the amount of fibronectin in the BSA solution, the amount of fibronectin adsorbed in the fibers should follow the same increase and there should be at least a statistically significant difference in the fluorescence intensity that depicts how much FN was absorbed and is available in the BSA fibers. Due to this unexpected results conclusion that the reason why these results were obtained may be due to the fact that during electrospinning, FN could have been denatured thus resulting in fibers that depicts no present of fibronectin as seen in *table 3.1* or the fact that even though the electrospun fibers have the same parameter, the density, thickness, amount of fibers and variability in fiber size each cover slip, available will still defer from other. We do not necessarily have the same amount of fibers so the BSA fibers with no FN may greater density or fiber than the fibers with high FN and vice versa.

Preliminary results prompted us to combat this issue posed by the fibers and be able to correctly quantify the amount of FN adsorbed in the BSA fibers which will allow us to know how cell adhesion is affected by the amount of FN available to bind to the integrins, BSA films were made. BSA films were made by taking 100 $\mu$ l of BSA solution with or without FN, depositing it on a cover slip and left to dry (1hr).

### 3.3.3 (TRIAL 2) Staining for Fibronectin in BSA Films

BSA films underwent ELISA staining using polyclonal antibody as done to the BSA fibers. In *Fig 3.2* the 6-well microtiter plate has three rows containing 0 $\mu$ g/ml FN, 1 $\mu$ g/ml FN and 10 $\mu$ g/ml FN. The top column is comprised of BSA films while the bottom column is comprised of BSA fibers. The column with the films shows that as the concentration of FN increased, there is a notable color change. So an increase in FN concentration results in an increase in the intensity detected by the spectrophotometer as depicted by the yellow color. The amount of light transmitted relates to the concentration of the fibronectin adsorbed into the sample.

The bottom column consisting of the BSA fibers does not visually show any color change which visually signifies any increase in the intensity of fibronectin. The spectrometer reading also supports the visual observation as supported in *table 3.1*.



FIGURE 3.2: 6-well plate of BSA films (top column) and BSA fibers (bottom column) of differing FN concentration.

### 3.3.3.1 (TRIAL 2) Results

The results obtained from the spectrometer reading supported our expected results. We made BSA films with varying amount of FN and expected that staining for the availability of fibronectin on the films will produce a data of fluorescence intensity that are significantly different. So a BSA film with a higher amount of fibronectin should have an intensity that is greater than BSA films with lower amount of available FN. In *fig 3.3*, we had three samples of BSA solution with varying amount FN (row 1, 2, 3) and a no sample control (row 4) which contained no BSA sample, no fibronectin, no polyclonal antibodies but only a substrate buffer (0.2M Tris Buffer + 5mM MgCl<sub>2</sub> in dH<sub>2</sub>O + p-Nitrophenyl phosphate tablets) solution and 3M NaOH stopping solution.

### 3.3.4 (TRIAL 3) Fibronectin Staining in BSA Films, Solvent Effect on Polyclonal FN Antibody Binding and on Monoclonal HFN7.1 Antibody Binding and Results

BSA films and fibers with varying amount of fibronectin were prepared to test TFE/H<sub>2</sub>O and PBS solvent effect on polyclonal fibronectin antibody binding which is not specific to one site on fibronectin and also on monoclonal antibody. The first step involved comparing the effect of TFE/H<sub>2</sub>O + BME solvent on polyclonal fibronectin antibody binding in BSA films (0FN, 1FN, 10FN) with effect of PBS solvent on the same polyclonal antibody. *Fig 3.3* shows that when BSA is dissolved in TFE/H<sub>2</sub>O + BME, as fibronectin availability in the BSA increased; there is a significant rise in the concentration of fibronectin adsorbed which under the analysis of variance a p-value of 0.00012 was obtained as seen in *table 3.3*. The significant level ( $\alpha$ ) was chosen to be 0.05. Since the p-value is less than the  $\alpha$ , indicating that the points were significantly different and we got an increase in antibody binding with an increase with FN in solution

which tells us there is an increase in the amount of FN there. However, the graph with the BSA polymer is dissolved in PBS produced a result depicting values of adsorbed fibronectin being less than zero. *Table 3.4* shows a p-value of 0.90718 which happens to be greater than 0.05 thus PBS points were not statistically significant.

The second step was to do the same comparison with both solvent but instead polyclonal antibodies were switched to monoclonal antibodies. Monoclonal antibodies (MAbs) are directed to cell attachment site indicating that the binding site is not disrupted and it has a high-affinity binding domain in fibronectin. The results gotten from here as seen in *fig 3.4* followed the same trend as when polyclonal antibodies were used with varying solvents. For TFE/H<sub>2</sub>O solvent, we got an increase in antibody binding with an increase with FN in solution which tells us there is an increase in the amount of FN there with a p-value of 0.00102 (*table 3.5*) which is less than the significant level (0.05) meaning that they are statistically significantly. However, there was more of an increase in the amount of FN adsorbed when monoclonal antibodies were used and this can be attributed to the fact that monoclonal antibodies are more active in protein confirmation and cell binding of FN is kept intact and not distorted. For PBS solvent, the p-value of 0.738 (*table 3.6*) was produced which because it is greater than the significant level means that points are not statistically significantly different.

The third step involved comparing the polyclonal fibronectin antibody in with monoclonal antibody binding in electrospun BSA fibers in TFE/H<sub>2</sub>O solvent. BSA fibers cannot be electrospun from PBS solvent. *Fig 3.5* shows a graph of polyclonal fibronectin antibody binding in electrospun BSA fiber and upon analyzing this graph; it presents us with a slight downward trend as there is an increase in FN concentration in the BSA

solution. The p-value is 0.54829 (*table 3.6*) (greater than the significant level of 0.05) meaning that the result is not a statistically significant difference. The signal did not vary significantly with the amount of fibronectin. We know that there is fibronectin but we cannot quantify the amount because of the significant difference in the BSA fibers.

*Fig 3.6* shows a graph of monoclonal fibronectin antibody binding in electrospun BSA fiber and upon analyzing this graph; it presents us a p-value of 0.95363 (*table 3.7*), the results as an increase in FN concentration in the BSA were not statistically different from each other just like the results obtained from monoclonal antibody binding in electrospun BSA fibers.

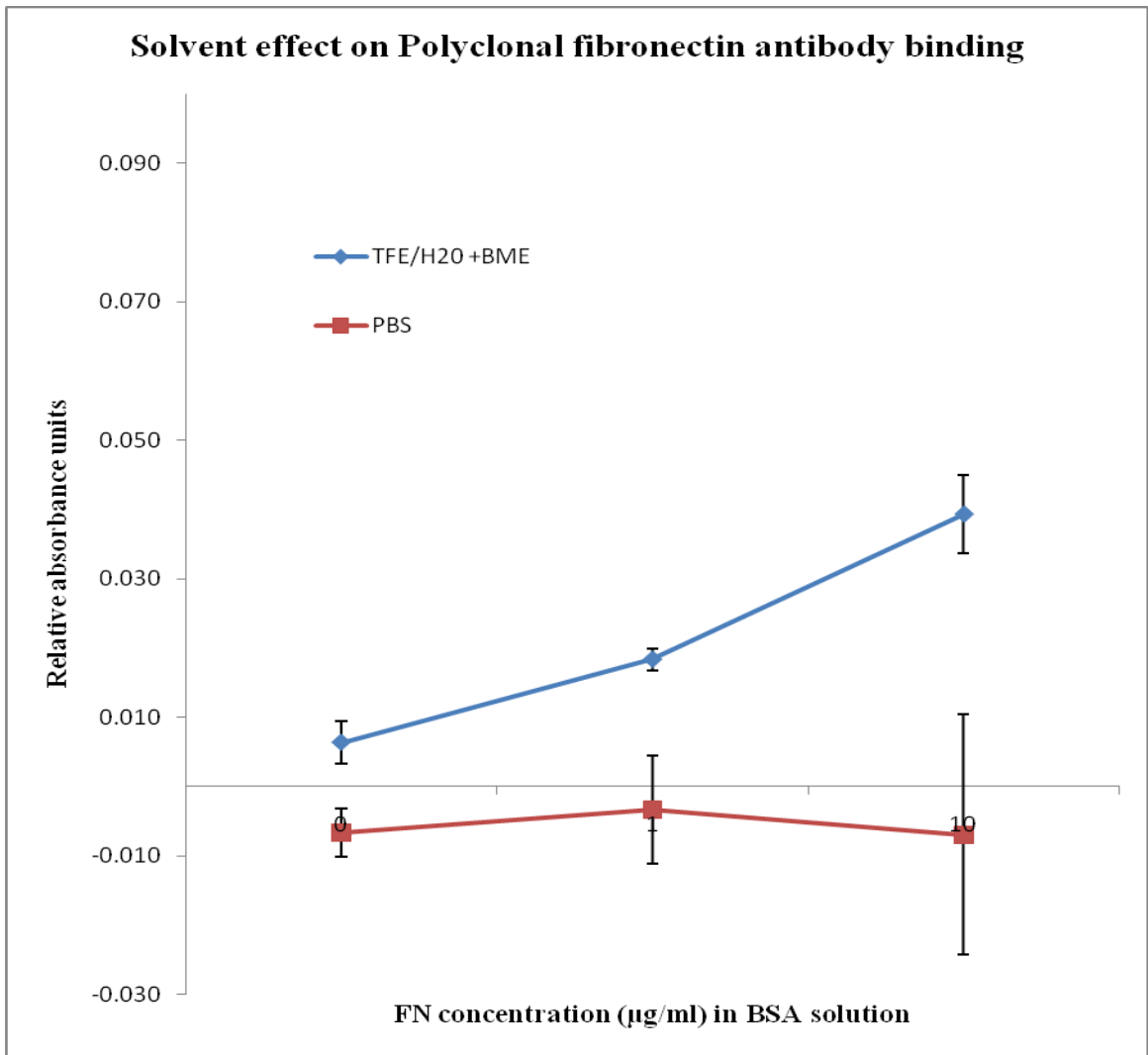


FIGURE 3.3: Solvent effect on polyclonal FN antibody binding

TABLE 3.2: Anova: Single factor analysis of TFE/H<sub>2</sub>O solvent effect on polyclonal FN antibody binding

<b>Anova: Single Factor (TFE/H<sub>2</sub>O)</b>						
SUMMARY						
<i>Groups</i>	<i>Count</i>	<i>Sum</i>	<i>Average</i>	<i>Variance</i>		
Column 1	3	0.019	0.00633	9.3E-06		
Column 2	3	0.055	0.01833	2.3E-06		
Column 3	3	0.118	0.03933	3.2E-05		
ANOVA						
<i>Source of Variation</i>	<i>SS</i>	<i>df</i>	<i>MS</i>	<i>F</i>	<i>P-value</i>	<i>F crit</i>
Between Groups	0.00167	2	0.00084	57.0682	0.00012	5.14325
Within Groups	8.8E-05	6	1.5E-05			
Total	0.00176	8				
<b>P-value is <math>\leq 0.05</math>. Statistically significant</b>						

TABLE 3.3: Anova: Single factor analysis of the PBS solvent effect on polyclonal FN antibody binding

<b>Anova: Single Factor (PBS)</b>						
SUMMARY						
<i>Groups</i>	<i>Count</i>	<i>Sum</i>	<i>Average</i>	<i>Variance</i>		
Column 1	3	-0.02	-0.0067	1.2E-05		
Column 2	3	-0.01	-0.0033	6E-05		
Column 3	3	-0.021	-0.007	0.0003		
ANOVA						
<i>Source of Variation</i>	<i>SS</i>	<i>df</i>	<i>MS</i>	<i>F</i>	<i>P-value</i>	<i>F crit</i>
Between Groups	2.5E-05	2	1.2E-05	0.09902	0.90718	5.14325
Within Groups	0.00075	6	0.00012			
Total	0.00077	8				
<b>P -value is <math>\geq 0.05</math>. Not statistically significant</b>						

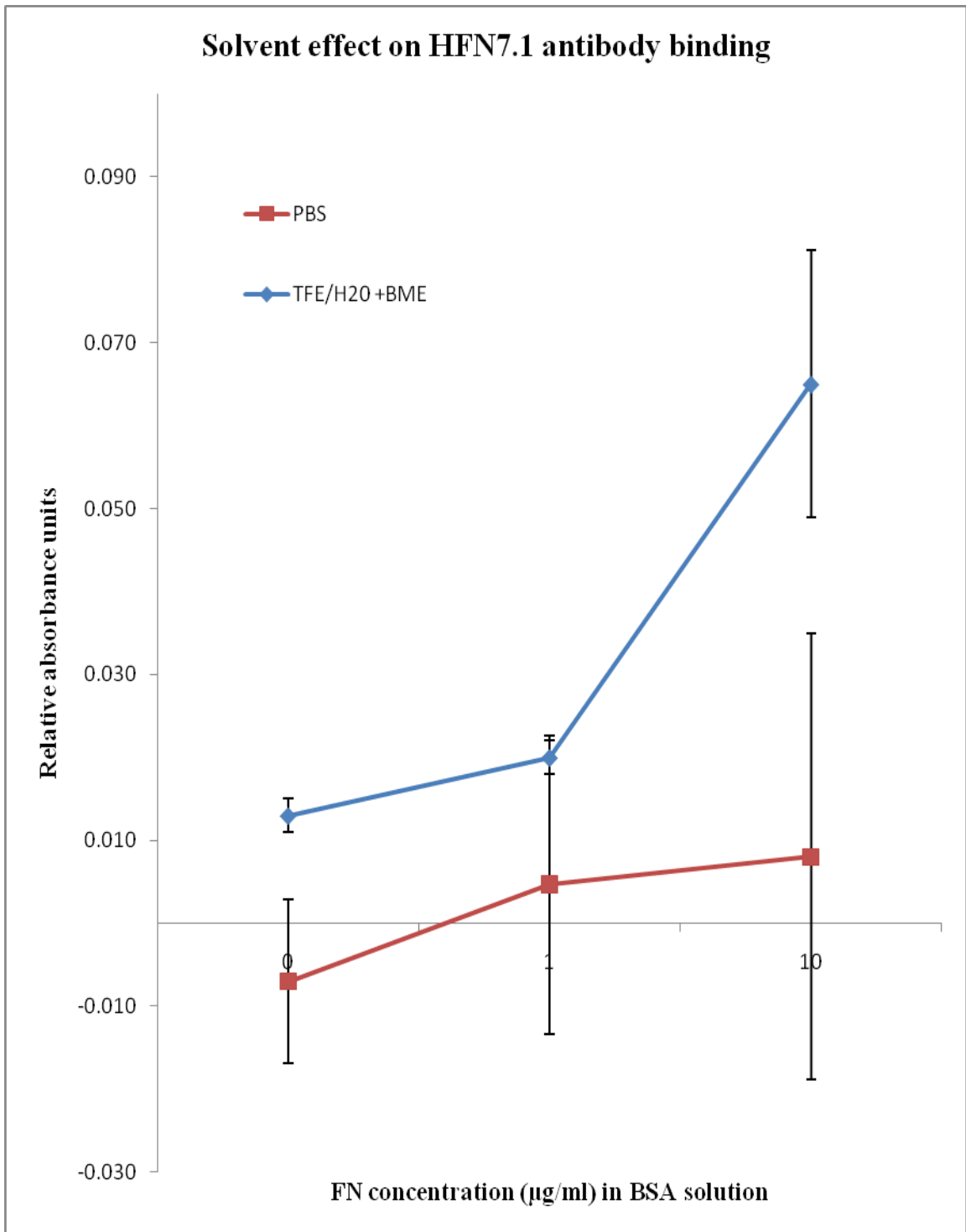


FIGURE 3.4: Solvent effect on HFN7.1 antibody binding

TABLE 3.4: Anova: Single factor analysis of TFE/H<sub>2</sub>O solvent effect on HFN7.1 antibody binding

**Anova: Single Factor (TFE)**

SUMMARY

<i>Groups</i>	<i>Count</i>	<i>Sum</i>	<i>Average</i>	<i>Variance</i>
Column 1	3	0.039	0.013	4E-06
Column 2	3	0.06	0.02	4E-06
Column 3	3	0.195	0.065	0.00026

ANOVA

<i>Source of Variation</i>	<i>SS</i>	<i>df</i>	<i>MS</i>	<i>F</i>	<i>P-value</i>	<i>F crit</i>
Between Groups	0.00478	2	0.00239	26.8427	0.00102	5.14325
Within Groups	0.00053	6	8.9E-05			
Total	0.00531	8				

**P-value  $\leq$  0.05. Statistically significant**

TABLE 3.5: Anova: Single factor analysis of PBS solvent effect on HFN7.1 antibody binding

**Anova: Single Factor (PBS)**

SUMMARY

<i>Groups</i>	<i>Count</i>	<i>Sum</i>	<i>Average</i>	<i>Variance</i>
Column 1	2	-0.014	-0.007	9.8E-05
Column 2	3	0.014	0.00467	0.00032
Column 3	3	0.024	0.008	0.00072

ANOVA

<i>Source of Variation</i>	<i>SS</i>	<i>df</i>	<i>MS</i>	<i>F</i>	<i>P-value</i>	<i>F crit</i>
Between Groups	0.00028	2	0.00014	0.32305	0.738	5.78614
Within Groups	0.00219	5	0.00044			
Total	0.00248	7				

**P -value is  $\geq$  0.05. Not statistically significant**

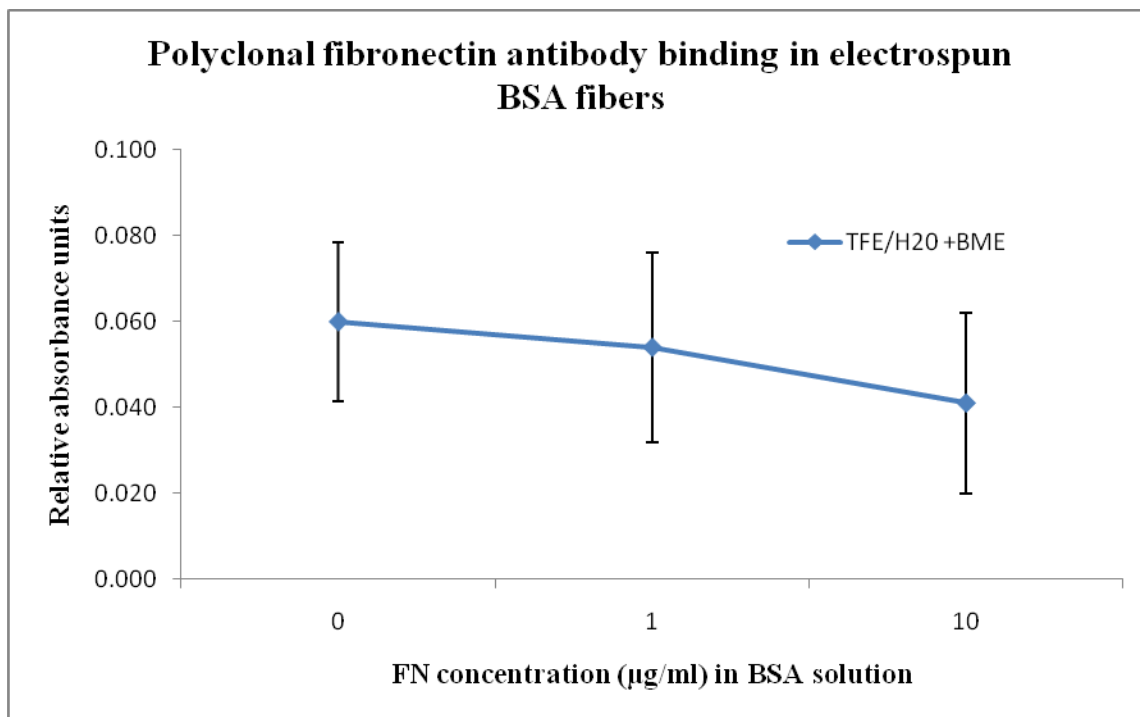


FIGURE 3.5: TFE/H<sub>2</sub>O solvent effect on polyclonal FN antibody binding on BSA fibers

TABLE 3.6: Anova: Single factor analysis of TFE/H<sub>2</sub>O solvent effect on polyclonal FN antibody binding on BSA fibers

<b>Anova: Single Factor</b>						
SUMMARY						
<i>Groups</i>	<i>Count</i>	<i>Sum</i>	<i>Average</i>	<i>Variance</i>		
Column 1	3	0.18	0.06	0.00034		
Column 2	3	0.162	0.054	0.00049		
Column 3	3	0.123	0.041	0.00045		
ANOVA						
<i>Source of Variation</i>	<i>SS</i>	<i>df</i>	<i>MS</i>	<i>F</i>	<i>P-value</i>	<i>F crit</i>
Between Groups	0.00057	2	0.00028	0.66536	0.54829	5.14325
Within Groups	0.00255	6	0.00043			
Total	0.00312	8				
<b>P -value is <math>\geq 0.05</math>. Not statistically significant</b>						

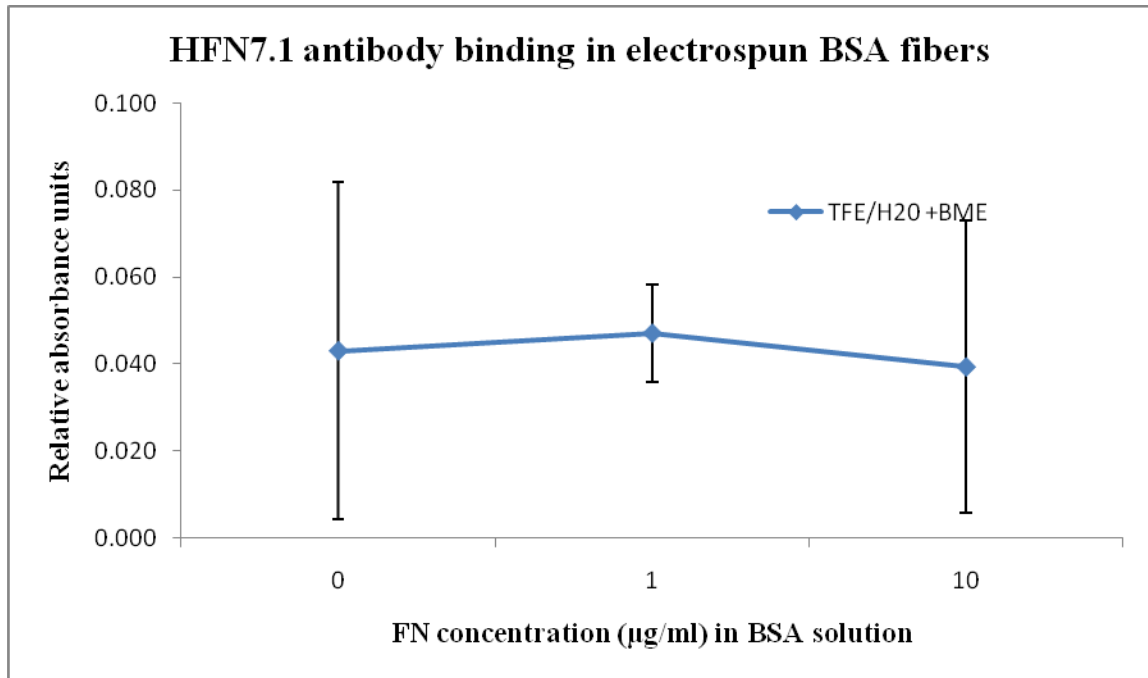


FIGURE 3.6: TFE/H<sub>2</sub>O solvent effect on polyclonal FN antibody binding on HFN7.1 antibody binding

TABLE 3.7: Anova: Single factor analysis of TFE/H<sub>2</sub>O solvent effect on HFN7.1 antibody binding on BSA fibers

<b>Anova: Single Factor</b>						
SUMMARY						
<i>Groups</i>	<i>Count</i>	<i>Sum</i>	<i>Average</i>	<i>Variance</i>		
Column 1	3	0.129	0.043	0.00151		
Column 2	3	0.141	0.047	0.00012		
Column 3	3	0.118	0.03933	0.00113		
ANOVA						
<i>Source of Variation</i>	<i>SS</i>	<i>df</i>	<i>MS</i>	<i>F</i>	<i>P-value</i>	<i>F crit</i>
Between Groups	8.8E-05	2	4.4E-05	0.04786	0.95363	5.14325
Within Groups	0.00553	6	0.00092			
Total	0.00562	8				
<b>P -value is <math>\geq 0.05</math>. Not statistically significant</b>						

### 3.4 CONCLUSION

We electrospun several fibers with varying amount of FN and expected that staining for the availability of fibronectin on the fibers will produce a data showing the concentration of FN adsorbed into the sample increase according to the initial amount of fibronectin that was available. However, the fibronectin signal did not vary significantly with the amount of fibronectin that is supposed to be adsorbed in the fibers. This is due to the even though they contain the same BSA concentration and the fibers were produced in the one process, the fibers with different FN concentration used to quantify the amount of FN adsorbed do not have the same amount of fibers and also will have a slight difference in their diameter. So we know that there is fibronectin available but we cannot quantify the amount because of the significant difference in the BSA fibers.

From the results obtained above, we can conclude that we cannot get a quantitative analysis of the amount of fibronectin adsorbed into a BSA fiber. Testing the hypothesis on whether the results from the BSA fibers have a statistically significant difference, a p-value of 0.54829 (*table 3.6*) which was greater the significant level ( $\alpha = 0.05$ ) meaning that the result is not a statistically significant difference and that the signal did not vary significantly with the amount of fibronectin. We know that there is fibronectin but we cannot quantify the amount because of the significant difference in the BSA fibers.

The only way to produce a quantitative or qualitative analysis or fibronectin adsorption will be through analysis it as films. As films, we were able to quantify the amount of fibronectin adsorbed and the results showed that there was a statistical difference between signals emitted by the fibronectin adsorbed meaning that not only do

we know that fibronectin was indeed adsorbed but we can also quantify the amount of fibronectin adsorbed. This quantification is very important as it serves as a baseline towards constructing a scaffold on which cells can adhere and we can compare how increasing the availability of fibronectin would affect cell adhesion and how we can quantify it.

Upon comparing PBS solvent effect on polyclonal fibronectin antibody binding and on monoclonal HFN7.1 antibody binding we found out that no matter the antibody used, the signals obtained showed no statistically significant difference. However, with the TFE/H<sub>2</sub>O there was rise in the amount of fibronectin adsorbed when compared to the amount of FN in the solution and the signal were statistically different.

## **CHAPTER 4: CELL ADHESION AND SPREADING ON SCAFFOLDS**

### **4.1 INTRODUCTION**

Cell adhesion is a complex biological process that involves receptor-ligands binding, stabilization by the actin cytoskeleton, and assembly of large intracellular protein complexes known as focal adhesions. Cell ECM adhesion is primarily mediated by the integrin family of transmembrane receptor (Hynes, 2002). Integrin-mediated adhesion to ECM proteins such as fibronectin and laminin, anchors cells to the ECM, provides structure to tissues, and triggers signals that control cell migration and survival (Mu Gao, Marcos Sotomayor, Elisabeth Villa, Eric Lee, and Klaus Schulten, 2006). This form of adhesion is a complex regulated process that involves interaction of receptors with ligand to promote cell spreading and strengthening of cell adhesion. As central elements in adhesion functioning, focal adhesions are protein complexes that functions as structural links to connect the extracellular matrix to the cell's cytoskeleton which triggers signaling pathways direction cell response (Mu Gao and Klaus Schulten, 2004).

In the focal adhesion complex, the mechanical and signaling processes are tightly coupled and analysis of the adhesion which provide important information for protein-function relationships for cell mediation proteins like fibronectin and structure function relationship for adhesive structures. A qualitative adhesion assay (BSA fibers and films

scaffolds, cell culturing and seeding) was developed to perform a quantitative and qualitative analysis of cell adhesion.

This present study analyzes adhesion strengthening and focal adhesion assembly on engineering BSA fibrous scaffolds and films that control the position and amount of cells adhering. By applying this electrospinning and film making technique, we were able to show control over the cell-substrate contact area and do a qualitative analysis of adhesion to biomimetic substrates. However, in our approach we are yet to perform a quantitative analysis of cells adhering to the electrospun fibers and fully equate adhesion strengthening and focal adhesion function. Performance of quantitative analysis of the adhesion strength provides us with a venue towards interpreting signaling focal adhesion components and comprehensive analysis of the biochemical interactions.

## **4.2 MATERIALS AND METHODS**

### **4.2.1 Cell Line and Culture Methods**

Embryonic fibroblast mouse cells (NIH/3T3) were used in this study. The NIH/3T3 cell line was grown in Dulbecco's Modified Eagle's Medium (DMEM) supplemented with 10% bovine calf serum and 1% penicillin streptomycin (Invitrogen). Culturing of the cells was conducted under sterile conditions in a sterile hood as an adherent monolayer requiring renewal of the medium and culturing every three days. For subculturing, the cells layer was rinsed with 0.25% (w/v) Trypsin-0.53mM EDTA solution to remove all traces of serum which contains the trypsin inhibitor. After rinsing, about 3.0ml of Trypsin-EDTA solution was added to the flask and the cells were observed under the microscope. To avoid clumping, the cells were not agitated by

shaking or continuous movement. Complete growth medium as added to the solution and the cells were aspirated followed by addition of appropriate aliquots of the cell suspension to new culture vessels. The aspirated cells were subcultured in a 1:3 ratio and at about an 80% confluence or less.

#### **4.2.2 Cell Counting**

Harvested cells were prepared for cell counting by putting 10 $\mu$ l of the cell in both sides of the hemocytometer. The number of cells was counted per square millimeter of the hemocytometer using a light microscope at 100X magnification. The concentration of the cell suspension was determined using the formula below:

$$\text{No. of cells per mL} = \# \text{ of cells counted per quadrant} * 10^4 \text{ cells/ml}$$

Total # of cells in the test tube used ( $C_{tt}$ ) = No. of cells/ml x Volume of test tube in which cells were suspended in ( $V_{tt}$ )

#### **4.2.3 Cell Staining**

The fluorescent dyes used for this experiment were rhodamine-phalloidin (red fluorescent dye) and Hoechst stain (blue fluorescent dye). The extracted cells were fixed in cold formaldehyde (3.7% formaldehyde in DPBS) for 5 minutes, permeabilized in Triton X (1% in DPBS) for 10 minutes, blocked in 1% bovine serum for 1 hour and incubated for 1 hour in rhodamine-phalloidin to stain for actin filaments and Hoechst to stain the nucleus.

### 4.3 RESULTS AND DISCUSSION

This project was designed to probe the effect of incorporating fibronectin into electrospun BSA fibers to support cell adhesion. To limit the issue of not being able to perform a quantitative analysis on cell adhesion on of BSA fibers whose results showed that all fiber scaffolds had no significant difference in their fluorescence intensity even though there was supposed to be different amount of fibronectin was incorporated to the BSA fibers, we came up with the idea of experimenting on thin BSA films. In the previous study, not only did we determine that BSA films were the sufficient matrix for quantifying the amount of adsorbed FN per differing concentration, we also determine that our best results was from use of monoclonal antibodies which were directed to the cell attachment site and have a high-affinity binding domain in fibronectin.

From previous shown ELISA studies we obtained results that showed that an increase in the amount of FN (0, 1 and 10 $\mu$ g per ml of BSA solution) available in a BSA solution made into a film scaffold resulted in signals which varied significantly with the amount of fibronectin adsorbed. We observed the presence of fibronectin and we were able to quantify the difference according to their varying concentration. To test the fact that BSA films should allow qualitative analysis of how FN availability increases cell adhesion, qualitative analysis of the differing amount of NIH/3T3 cells adhered to the surface (film and fiber) when exposed to varying amount of adsorbed FN was conducted.

*Fig 4.1 a, b and c* shows us a visual image of cells adhering to the BSA film with TFE/H<sub>2</sub>O as its solvent. The films cast from TFE/H<sub>2</sub>O were a translucent thick multilayer gel of proteins and the number of cells that adhered to the film increased with an increase in the amount of FN (0, 1 and 10 $\mu$ g/ml). We can also see that the actin

filaments were spread to the same extents in all the films. In the cells that adhere to the films with lower concentration, they were not uniformly dispersed and were seen in clusters. However, an increase in FN concentration brought about a uniform distribution all aligned in a particular direction. The evidence provided here also shows us how cell adhesion modulates cell behavior with the clustering of cells in a scaffold with lower FN concentration and spreading of cells in a scaffold with higher FN concentration.

*Fig 4.2 a, b and c* shows us a visual image of cells adhering to the BSA film with PBS as its solvent. From the images we can note that an increase in the amount of FN did not lead to an increase in the number of cells that adhered to the surface. These results support the quantitative analysis of TFE/H<sub>2</sub>O vs. PBS solvent effect on antibody binding from the previous chapter. ELISA indicated that there no FN was detected on BSA surface from PBS/BSA solution but cells did adhere. This adhesion is as a result of serum proteins being adsorbed to the bare regions of the surface despite BSA blocking.

*Fig 4.3* shows a visual image of the NIH/3T3 cells adhering to 10µg/ml FN film diluted in TFE/H<sub>2</sub>O solvent. As expected, there was an increase amount of cells that adhered to the surface with increasing FN solution concentration. In this case, the film is much thicker, which likely prevents nonspecific serum protein adsorption to the surface. It is noteworthy, however, that a basal level of cell adhesion was observed in films made from FN free BSA solution in TFE/H<sub>2</sub>O. This correlates well with the ELISA results. We hypothesize that this could be due to some protein adsorption to the denatured BSA. Further experiments are required to verify this.

*Fig 4.4* shows a visual image of the cells adhering to electrospun BSA fibers. Here, we can immediately notice the cell adhering to the fibers and sticking in direction

of the fiber alignment. We observed cell adhesion to all fibers. It appears that fewer cells attached to fibers without incorporated FN, but due to the variability in fiber density it is difficult to quantify.



FIGURE 4.1 (a): NIH/3T3 cells adhering to BSA film (TFE/H<sub>2</sub>O solvent) with 0 $\mu$ g/ml FN (10x). Pic shows nucleus (blue).

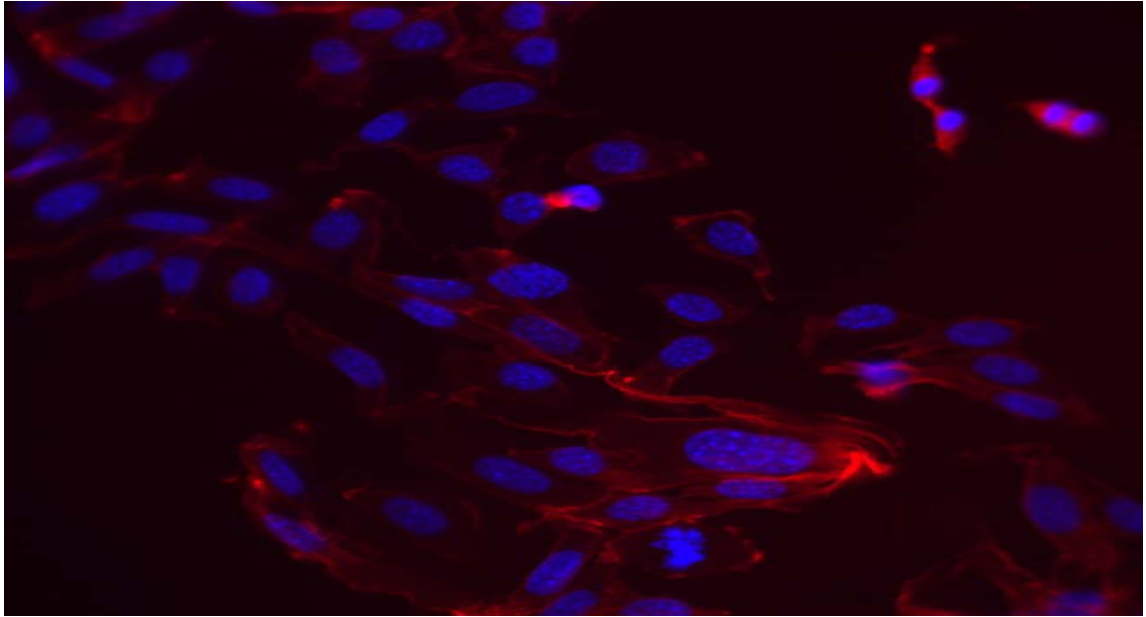


FIGURE 4.1 (b): NIH/3T3 cells adhering to BSA film (TFE/H<sub>2</sub>O solvent) with 1 $\mu$ g/ml FN. Pic shows both actin filaments (red) and nucleus (blue).

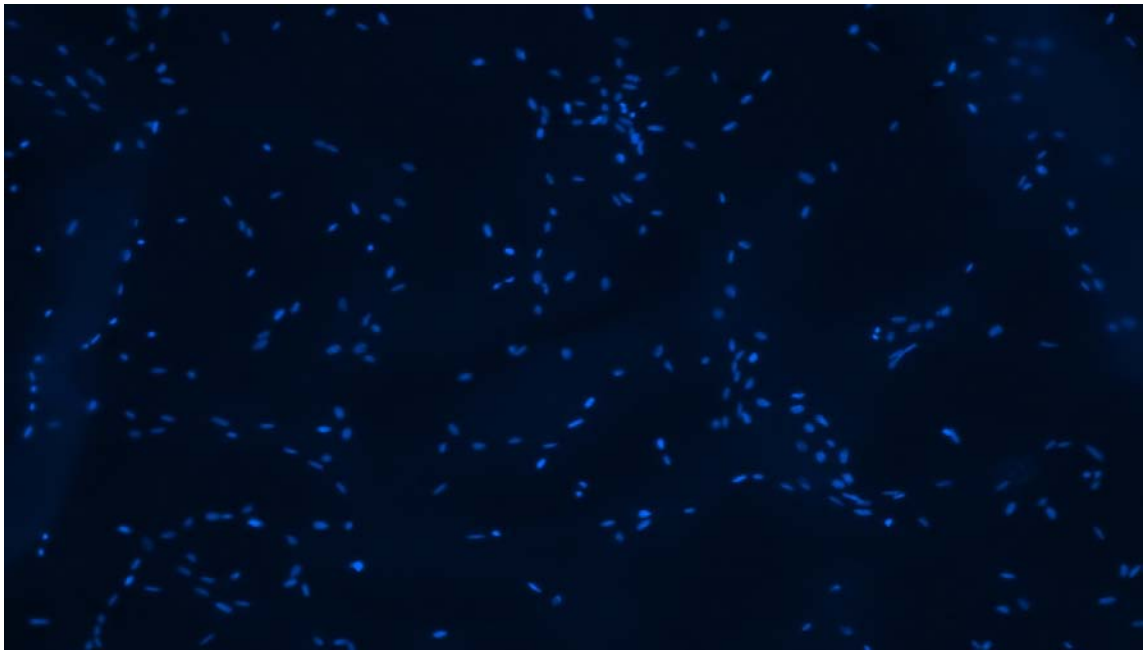


FIGURE 4.1 (c): NIH/3T3 cells adhering to BSA film (TFE/H<sub>2</sub>O solvent) with 10 $\mu$ g/ml FN. Pic shows nucleus (blue).

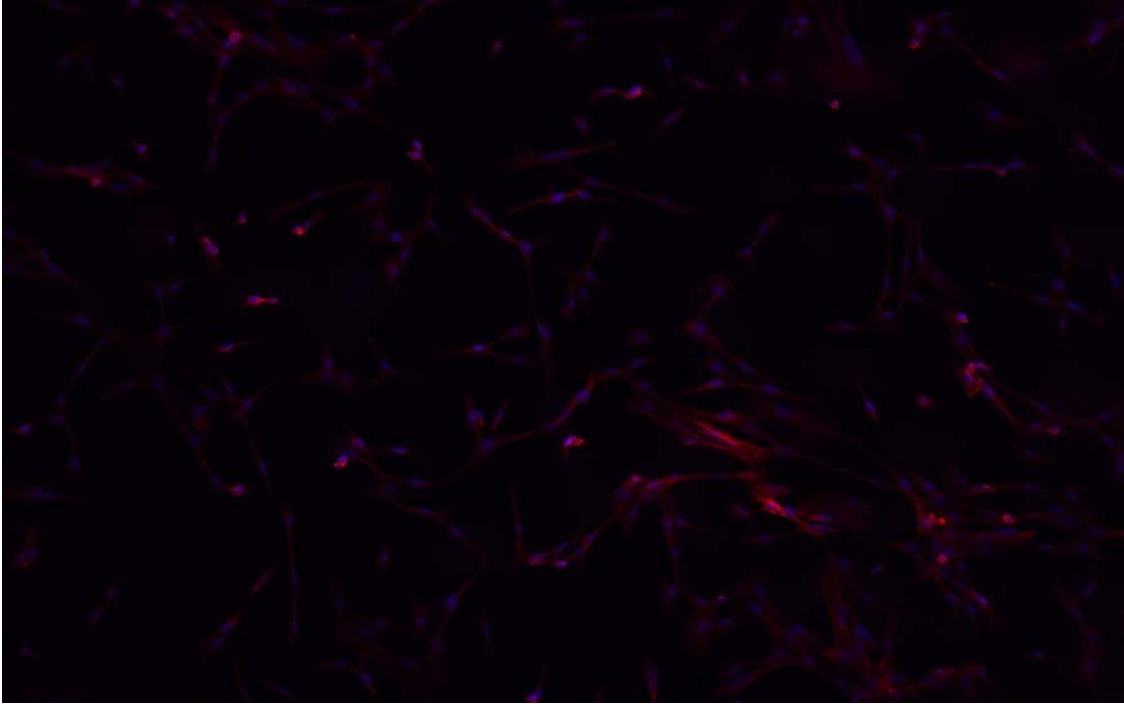


FIGURE 4.2 (a): NIH/3T3 cells adhering to BSA film (PBS solvent) with 0 $\mu$ g/ml FN

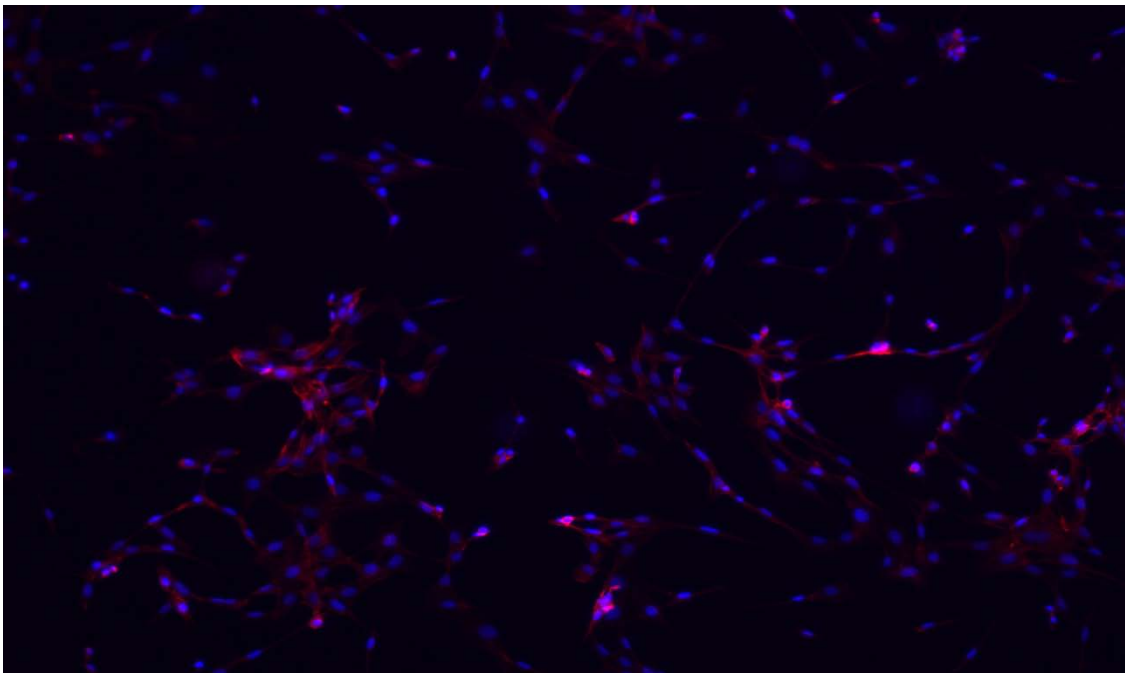


FIGURE 4.2 (b): NIH/3T3 cells adhering to BSA film (PBS solvent) with 1 $\mu$ g/ml FN

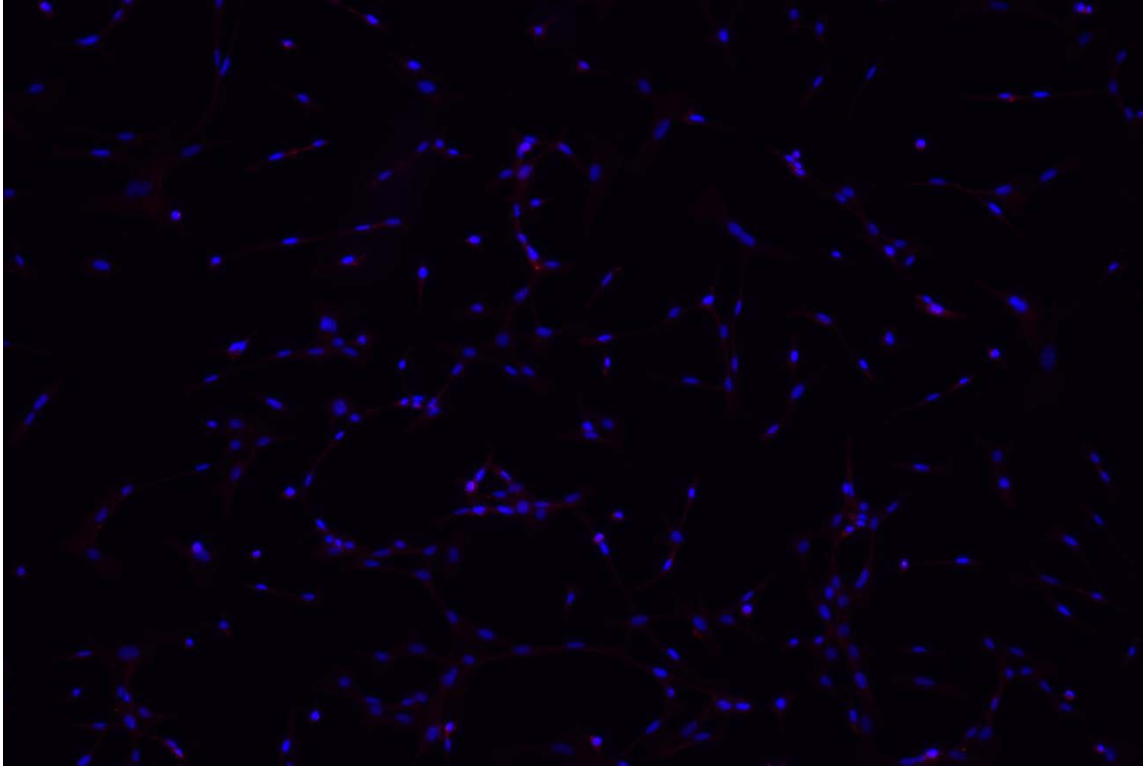


FIGURE 4.2 (c): NIH/3T3 cells adhering to BSA film (PBS solvent) with 10 $\mu$ g/ml FN

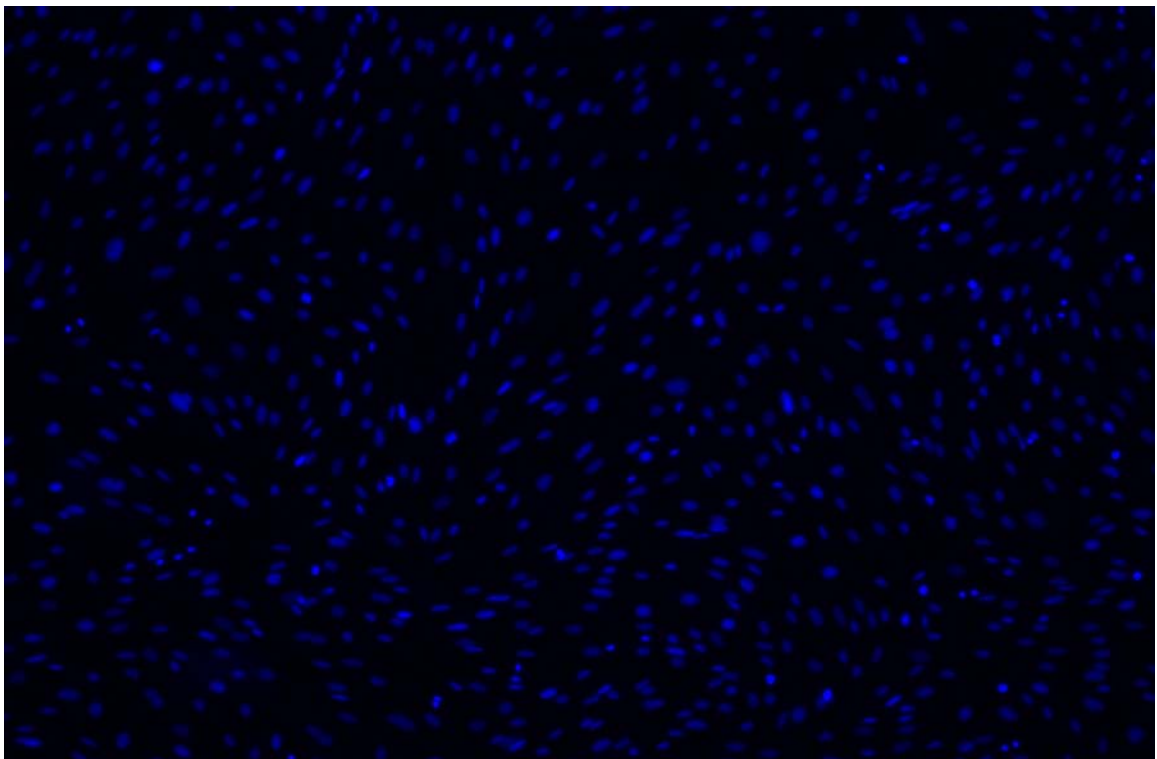
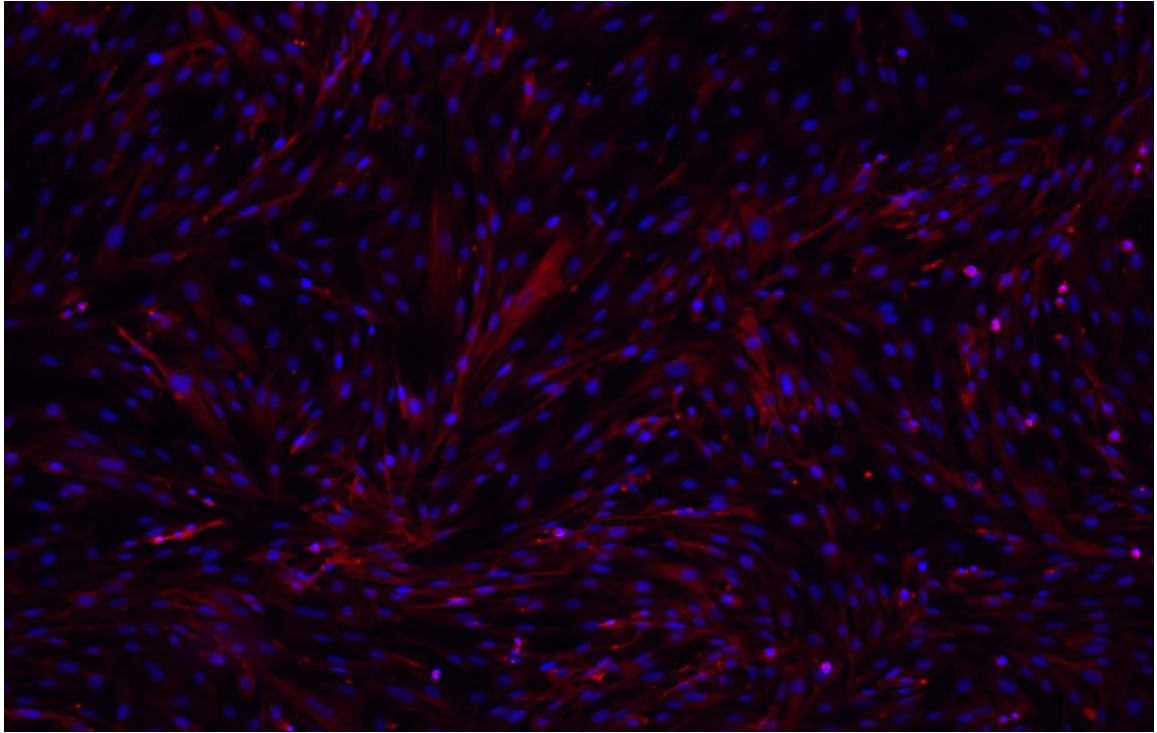


FIGURE 4.3: NIH/3T3 cells adhering to 10 $\mu$ g/ml FN film diluted in TFE/H<sub>2</sub>O solvent (10x). Top pic shows both nucleus (blue) and actin filament (red). Bottom shows just nucleus

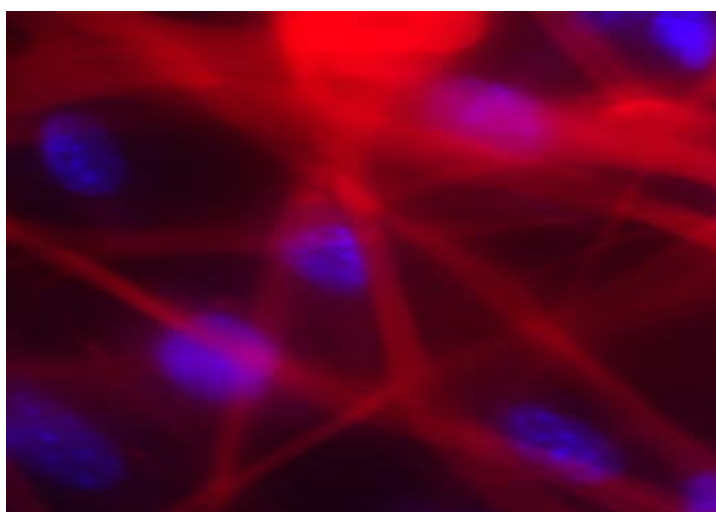
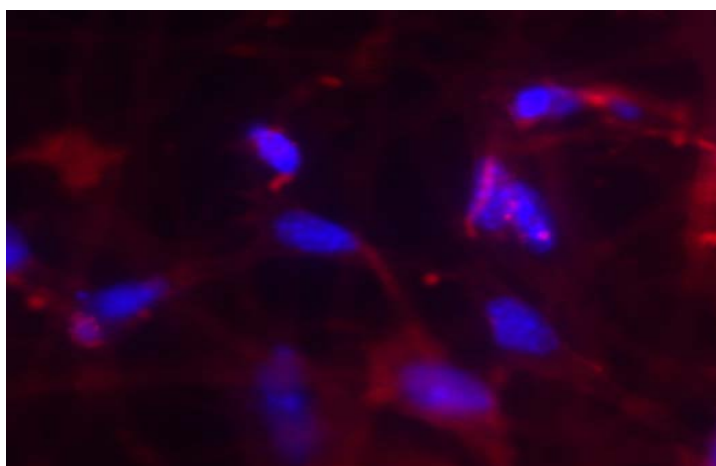
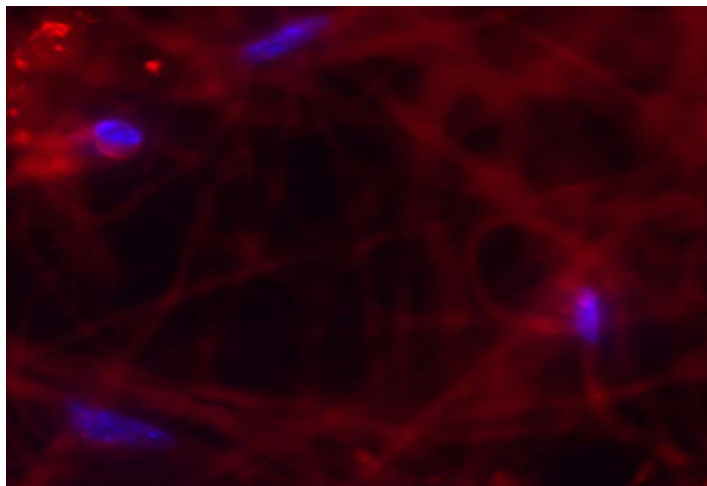


FIGURE 4.4: NIH/3T3 cells adhering to BSA fibers (TFE/H<sub>2</sub>O solvent) (10x). (a) fiber with 0 μg/ml FN, (b) fiber with 1 μg/ml FN, (c) fiber with 0 μg/ml FN. Pics show both actin filaments (red) and nucleus (blue).

#### **4.4 CONCLUSION**

The use of BSA fibers and films to support cell adhesion and control cell spreading allowed us to quantitatively analyze fibronectin activity through the BSA films which in turn provided us with an avenue to predict the effect it will have on cell adhesion and qualitatively examine the contribution of FN and focal adhesion assembly to cell adhesion. The adhesion comparison for the NIH/3T3 fibroblast cells that were seeded on the several BSA fibers was barely dependent on the amount of FN adsorbed in the fibers but more on the physiological components that differ each fiber surface from the other even though the fibers were produced in the same run on the same target. The restriction was in the variability in fiber density that was placed in the several selected areas of the target which we used for FN adsorption comparison. This fiber variation made it is difficult to quantify cell adhesion.

## **CHAPTER 5: PROJECT SUMMARY AND FUTURE CONSIDERATION**

The overall goals of this project are to develop a biomimetic scaffolds and investigate how cell adhesion modulates cell behavior in 3-dimensional culture. Bovine serum albumin (BSA) also known as was “Fraction V” and which has a human analogue (human serum albumin) was selected for the scaffold due to its stability, low cost, advantageous biochemical and biotechnological application such as a nonadhesive blocking agent, in immunoassays or as an enzymatic stabilizer, and more importantly due to the assumption that being one of the most abundant protein in the body, nanofibers electrospun from this globular protein would be biocompatible and not be rejected by the body by being considered less foreign (Peters, T 1995). It was hypothesized that cell adhesion, function and differentiation can be controlled by varying the amount of fibronectin in non-adhesive fiber matrices.

To extend our knowledge of cell adhesion to a more relevant 3D culture, we engineered electrospun nanofibers designed to mimic the extracellular matrix and control cell adhesion. This model allowed us to engineer the diameter, pore size, chemistry and surface topography of the electrospun scaffold through optimization of its parameters to achieve an efficient biodegradable and biocompatible matrix. This experimental system allowed us to independently manipulate the electrospinning parameters within the framework of our experimental system providing us with trends that supported empirical

observation of these studies through the fiber morphology and other research findings. A method that was adapted so that cells could have adhesive structures on which adhesion can be controlled. This framework can still be reworked and used as a predictive tool to guide future experimental analysis.

The next step involved conducting a quantitative biochemical assay, an ELISA, to measure the absorption of an enzymatic product which correlates to the fibronectin specific antibody binding in the electrospun fibers and BSA films. The measurement of absorbance at 405 nm indicated an increase in the films comparison directly proportional to the amount of FN adsorbed in the films. This trend was not equivalent to what was observed in the BSA fibers which showed no statistical significant difference in the ELISA even though there was supposed to be based on the fact that different amount of fibronectin was incorporated to the BSA fibers. Our expected results was that by increasing the amount of fibronectin in the BSA solution, the amount of fibronectin adsorbed in the fibers should follow the same increase and there should be at least a statistically significant difference in the fluorescence intensity that depicts how much FN was absorbed and is available in the BSA fibers. These results prompted a means to quantify the amount of FN adsorbed in the BSA fibers which will allow us to know how cell adhesion is affected by the amount of FN available to bind to the integrins. This means was satisfied by doing a quantitative analysis on BSA films that have equivalent surface area. The result from cell adhesion analysis agreed with our experimental measurement of the ELISA absorbance which gave us both a quantitative and qualitative analysis of how fibronectin can affect cell adhesion strengthening.

In conclusion, we have obtained a qualitative analysis of cell adhesion on electrospun scaffolds and how cell adhesion modulates cell behaviors as a function of adhesive area, focal adhesion and fibronectin composition. By combining the BSA surfaces with quantitative measurement of fibronectin fluorescence intensity coupled with a qualitative cell adhesion assay. However, in our approach we are yet to perform a quantitative analysis of cells adhering to the electrospun fibers and fully equate adhesion strengthening and focal adhesion function.

In the future, performing a quantitative analysis of the adhesion strength will provide us with a venue towards interpreting signaling focal adhesion components and comprehensive analysis of the biochemical signals triggered by adhesion to this scaffold.

This is an innovative research project because of the integration of quantitative assays and ECM mimicked structures (protein fibers and films) to manipulate cell adhesion in order to modulate cell behavior as a function of adhesive area, focal adhesion and fibronectin composition. A procedure that was achieved by combining the BSA surfaces with quantitative measurement of fibronectin fluorescence intensity coupled with a qualitative cell adhesion to analyze the structure-function and protein –function of the adhesion complexes. This approach has provided insights into developing an understanding of cell how adhesion plays a significant role in the field of tissue engineering that aims in the production of tissue substitutes from biodegradable and biocompatible polymers and cells that are specific for the tissues.

For further study, with findings from our experiments which showed that denatured BSA does enhance cell adhesion but regular globular protein prevents it we can be able to modulate cell adhesion by making fibers through denatured BSA and

coating it with undenatured globular BSA. A strategy that include decorating the BSA surface with glutaraldehyde, a amine-reactive homo-bifunctional cross-linker which will bind the amine group on the denatured BSA scaffold with the cross linker having a free amine binding group that would be available to bind to the undenatured BSA globular protein. Thus coating the surface and modulating cell adhesion. To further advance this work in the future, further reduction of the nonspecific binding of serum protein to the scaffold would be needed for quantitative analysis of cell adhesion from the electrospun BSA scaffold. Measurement of the adhesion strength would also be needed to give the structure-function information about adhesion mechanism.

## REFERENCES

- Alkiyama, S.K., Yamada, S. S., Chen, W. T. and Yamada, K. M. (1989). *Analysis of fibronectin receptor function with monoclonal antibodies: Roles in cell adhesion, migration, matrix assembly, and cytoskeleton organization*. J. Cell Biol. 109, 863-875.
- Anderson, J.M., Bonfield, T.L., and Ziats, N.P. (1990). *Protein adsorption and cellular adhesion and activation on biomedical polymers*. Int J Artific Organs 13, 375-382.
- Baumgarten P. (1971). *Electrostatic spinning of acrylic microfibers*. J Colloid InterfaceSci; 36(1):71-9.
- Baron M. Main AL. Driscoll PC. Mardon HJ. Boyd J. Campbell ID (1992). *<sup>1</sup>H NMR Assignment and Secondary Structure of the Cell Adhesion Type III Module of Fibronectin*. 31: 2068-2073
- Bhattacharai, S.R., Bhattacharai, N., Yi, H.K., Hwang, P.H., Kim, H.Y. (2004). *Novel biodegradable electrospun membrane: Scaffold for tissue engineering*. Biomaterials 25, 2595.
- Chen, C. Cao, C. Ma, X. Tang, Y. Zhu, H.S (2006). Polymer 47, 6322-6327.
- Darell H. Reneker, and Alexander L. Yarin (2008). *Electrospinning jets and polymer nanofibers*. Polymer. Volume 49, Issue 10, Pages 2387-2425.
- David Craig, Mu Gao, Klaus Schulten, and Viola Vogel (2004). *Structural insights into how the MIDAS ion stabilizes integrin binding to an RGD peptide under force*. Structure, 12:2049-2058, 2004.
- De Arcangelis, A. and Georges-Labouesse, E. (2000). *Integrin and ECM function: roles in vertebrate development*. Trends Genet 16, 389-395.
- Hayati I, Bailey AI, Tadros TF (1987). *Investigations into the mechanisms of electrohydrodynamic spraying of liquids. 1. Effect of electric-field and the environment on pendant drops and factors affecting the formation of stable jet and atomization*. J Colloid Interface Sci May; 117(1):205-21.

- Hohman, M.M., Shin, M., Rutledge, G., Brenner, M.P. (2001). *Electrospinning and electrically forced jets: Stability theory*. Phys. Fluids 13, 2201.
- J. Doshi and D.H. Reneker (1995). *Electrospinning process and applications of electrospun fibers*. J Electrostatics. 35 (2-3): 151-60.
- J.M. Deitzel, J. Kleinmeyer, D. Haris et al., (2001). *The effect of processing variables on the morphology of electrospun nanofibers and textiles*. Polymer Jan; 42 (1): 261-72
- J.M. Deitzel, N.C. Beck Tan, J.D. Kleinmeyer et al., (1999). Report No. ARL-TR-1989.
- Kristin J. Pawlowski, Catherine P. Barnes, Eugene D. Boland, Gary E, Wnek and Gary L. Bowlin (2004). *Biomedical Nanoscience: Electrospinning Basic Concept, Application, and Classroom Demonstration*. Mat. Res. Soc. Symp. Proc. Vol 827E.
- Lotz, M.M., Budsal, C.A., Erickson, H.P., McClay, D.R. (1989). *Cell adhesion to fibronectin and tenascin: Quantitative measurements of initial binding and subsequent strengthen response*. J. Cell Biol. 109, 1795-1805.
- Mathews JA, Wnek GE, Simpson DG, Bowlin GI (2002). *Electrospinning of collagen nanofibers*. Biomacromolecules 3:232-8.
- Megelski S. Stephens JS. Chase DB, Rabolt JF (2002). *Micro-and nanostructured surface morphology on electrospun polymer fibers*. Macromolecules Oct 22; 35(22):8456-66.
- M. Bognitzki, T. Frese, J.H. Wendorff et al. (2000). *Abstracts of Papers of the American Chemical Society*. 219, U419.
- Mu Gao, Marcos Sotomayor, ELISAbeth Villa, Eric Lee, and Klaus Schulten (2006). *Molecular mechanisms of cellular mechanics*. Physical Chemistry - Chemical Physics, 8:3692-3706.
- Peters, T (1995). *All about Albumin: biochemistry, Genetics and Medical Applications*. Academic Press: new York.
- Potts JR and Campbell ID. (1994). *Fibronectin Structure and Assembly*. Curr. Cell Bio. 6: 648-655.
- Potts JR and Campbell ID (1996). *Structure and Function of Fibronectin Modules*. Matrix Bio. 15: 313-320.
- Reneger, D. H, Yarin, A.L, Zussman, E. Xu (2007). *Adv. Appl. Mech.* 41, 43-195.

- R. Jaeger, M.M. Bergshoef, C.M.I Batlle et al., (1998). *Electrospinning of ultra-thin polymer fibers*. Macromolecular Symposia 127: 141-50.
- Shin, H. J, Lee, C.J, Cho, I.H, Kim, Y.J et al (2006). *J. biomater. Sci. Polymer Ed.* 26, 2603-2610.
- Souheil Zekri, Rahul Singhal, Nick Baksh and Ashok Kumar (2006). *Electrospinning of Micro and Nano fibers for Biomedical Applications*. Nanomaterials and Nanomanufacturing Research Center , 167.
- Taylor G (1969). *Electrically driven jets*. Proc Natl Acad Sci London; A313(1515):453-75.
- Thomas, E. Heine, E. Wollseifen, R. Cimpeanu, C. Moller , M (2005). *Int. Nonwovens*. 14, 12- 18.
- Thomas PD, Dill KA. (1993). *Local and nonlocal interactions in proteins and mechanisms of alcohol denaturation*. Protein Sci 2:2050–2065.
- Travis J. Sill and Horst A. Von Recum. (2008). *Electrospinning: Applications in Drug delivery and tissue engineering*. Biomaterials 29, 1989-2006.
- Yarin AL, Koombhongse S. Reneker DH (2001). *Bending instability in electrospinning nanofibers*. J Appl Physics Mar 1;89(5):3018-26.
- Yael Dror, Tamar Ziv, Vadim Makarov, Hila Wolf, Arie Admon and Eyal Zussman. (2008). *Nanofibers made of Globular Proteins*. Biomacromolecules, 9, 2749-2754.
- Zarkoob, S. Eby, R. Reneker, D.H. Hudson, S.d., Ertly, D. Adams, W.W. (2004). *Polymer* 45, 3973-3977.